

## Optimization of 2-anilino 4-amino substituted quinazolines into potent antimalarial agents with oral in vivo activity

Paul R Gilson, Cyrus Tan, Kate E. Jarman, Kym N. Lowes, Joan M. Curtis, William Nguyen, Adrian E. Di Rago, Hayley E. Bullen, Boris Prinz, Sandra Duffy, Jonathan B. Baell, Craig A Hutton, Helene Jousset Sabroux, Brendan S. Crabb, Vicky M. Avery, Alan F. Cowman, and Brad E. Sleebs

*J. Med. Chem.*, **Just Accepted Manuscript** • DOI: 10.1021/acs.jmedchem.6b01673 • Publication Date (Web): 12 Jan 2017

Downloaded from <http://pubs.acs.org> on January 12, 2017

### Just Accepted

“Just Accepted” manuscripts have been peer-reviewed and accepted for publication. They are posted online prior to technical editing, formatting for publication and author proofing. The American Chemical Society provides “Just Accepted” as a free service to the research community to expedite the dissemination of scientific material as soon as possible after acceptance. “Just Accepted” manuscripts appear in full in PDF format accompanied by an HTML abstract. “Just Accepted” manuscripts have been fully peer reviewed, but should not be considered the official version of record. They are accessible to all readers and citable by the Digital Object Identifier (DOI®). “Just Accepted” is an optional service offered to authors. Therefore, the “Just Accepted” Web site may not include all articles that will be published in the journal. After a manuscript is technically edited and formatted, it will be removed from the “Just Accepted” Web site and published as an ASAP article. Note that technical editing may introduce minor changes to the manuscript text and/or graphics which could affect content, and all legal disclaimers and ethical guidelines that apply to the journal pertain. ACS cannot be held responsible for errors or consequences arising from the use of information contained in these “Just Accepted” manuscripts.

1  
2  
3 **Optimization of 2-Anilino 4-Amino Substituted**  
4  
5  
6 **Quinazolines into Potent Antimalarial Agents with Oral in**  
7  
8  
9  
10 **Vivo Activity**  
11  
12  
13  
14  
15  
16  
17

18 Paul R. Gilson,<sup>⊥,#</sup> Cyrus Tan,<sup>†,‡</sup> Kate E. Jarman,<sup>†,‡</sup> Kym N. Lowes,<sup>†,‡</sup> Joan M. Curtis,<sup>†</sup>  
19  
20 William Nguyen,<sup>†,‡</sup> Adrian E. Di Rago,<sup>†</sup> Hayley E. Bullen,<sup>⊥</sup> Boris Prinz,<sup>⊥</sup> Sandra  
21  
22 Duffy,<sup>§</sup> Jonathan B. Baell,<sup>€</sup> Craig A. Hutton,<sup>¥</sup> Helene Jousset Subrox,<sup>†,‡</sup> Brendan S.  
23  
24 Crabb,<sup>⊥,#,‡</sup> Vicky M. Avery,<sup>§</sup> Alan F. Cowman,<sup>†,‡</sup> and Brad E. Sleebs.<sup>†,‡,\*</sup>  
25  
26  
27  
28  
29

30 <sup>†</sup>The Walter and Eliza Hall Institute of Medical Research, Parkville 3052, Australia  
31  
32

33 <sup>‡</sup>Department of Medical Biology, The University of Melbourne, Parkville 3010, Australia  
34  
35

36 <sup>€</sup>Monash Institute of Pharmaceutical Sciences, Monash University, Parkville, Victoria, 3052, Australia.  
37  
38

39 <sup>¥</sup>School of Chemistry and Bio21 Molecular Science and Biotechnology Institute, University of  
40  
41 Melbourne, Parkville, VIC 3010, Australia  
42  
43  
44

45 <sup>§</sup>Discovery Biology, Eskitis Institute for Drug Discovery, Griffith University, Nathan, Queensland  
46  
47 4111, Australia  
48  
49

50 <sup>⊥</sup>Macfarlane Burnet Institute for Medical Research and Public Health, Melbourne, 3004, Australia.  
51  
52

53 <sup>#</sup>Monash University, Clayton, Victoria, 3800, Australia.  
54  
55  
56  
57  
58  
59  
60

1  
2 \*Correspondence to:

3  
4 Brad E. Sleebs

5  
6 The Walter and Eliza Hall Institute of Medical Research

7  
8 1G Royal Parade, Parkville 3052, Victoria, Australia

9  
10  
11 Phone: 61 3 9345 2718

12  
13  
14 Email: [sleebs@wehi.edu.au](mailto:sleebs@wehi.edu.au)

15  
16  
17  
18  
19  
20 **KEYWORDS**

21 Malaria, *Plasmodium*, antimalarial, quinazoline.

22  
23  
24  
25  
26  
27 **ABSTRACT**

28  
29  
30 Novel antimalarial therapeutics that target multiple stages of the parasite lifecycle are urgently  
31 required to tackle the emerging problem of resistance with current drugs. Here we describe the  
32 optimization of the 2-anilino quinazoline class as antimalarial agents. The class, identified from  
33 publicly available antimalarial screening data, was optimized to generate lead compounds that possess  
34 potent antimalarial activity against *P. falciparum* parasites comparable to the known antimalarials,  
35 chloroquine and mefloquine. During the optimization process we defined the functionality necessary  
36 for activity and improved *in vitro* metabolism and solubility. The resultant lead compounds possess  
37 potent activity against a multi-drug resistant strain of *P. falciparum* and arrest parasites at the ring  
38 phase of the asexual stage and also gametocytogenesis. Finally, we show that the lead compounds are  
39 orally efficacious in a 4 day murine model of malaria disease burden.  
40  
41  
42  
43  
44  
45  
46  
47  
48  
49  
50  
51  
52  
53  
54  
55  
56  
57  
58  
59  
60

## INTRODUCTION

Malaria is a life-threatening disease caused by infection with protozoan parasites of the genus *Plasmodium*. Each year *Plasmodium* parasites cause over two hundred million infections and over 438,000 deaths, predominantly children.<sup>1</sup> The two most lethal forms of malaria are caused by infection with either *P. falciparum*, which is hyper-endemic in Africa and the most deadly parasite, or *P. vivax*, responsible for recrudescence infection via activation of dormant liver-stage hypnozoites that re-establish the clinical blood-stage of infection.<sup>2</sup>

Preventive interventions against malaria, such as bed nets, insecticide spraying, removal of stagnant water from living areas and improved access to therapies has considerably reduced the global incidence of malaria since the turn of the century; however, malaria is still an enormous problem throughout the world, and particularly in Africa. While antimalarial agents, such as chloroquine, have been used successfully to treat millions of malaria infections, the emergence and spread of chloroquine resistance necessitated the introduction of combination therapies of mefloquine, atovaquone, and artemisinin analogues.<sup>3</sup> Despite this, resistance to artemisinin-based combination therapies has now been reported along the Thai-Cambodian border and has potential to spread.<sup>4</sup> The continual emergence of resistant plasmodial strains of malaria highlights the urgent need for the development of new antimalarial therapies against novel targets.

To combat the onset of resistance, the WHO has stipulated that new classes of drugs should possess activity against multiple stages of the parasite's lifecycle. To catalyse the identification of these agents, Medicines for Malaria Venture (MMV) recently encouraged industry and academic medical research institutes to conduct phenotypic high throughput screens (HTS) using their internal and proprietary compound libraries to identify compounds that not only reduced asexual stage parasite viability but also acted on liver and sexual blood stage parasites. Over the last 10 years several high throughput

1  
2 screens have been undertaken by various organisations<sup>5-9</sup> and the data from these screens have been  
3  
4 made publicly available to the research community.  
5  
6

7  
8 We used this resource to identify a small molecule starting point that demonstrated activity across  
9  
10 multiple stages of the parasites lifecycle. In identifying this starting point, we also took into  
11  
12 consideration other important attributes such as activity against parasite lines with resistance to known  
13  
14 antimalarials, cytotoxicity profile, chemical liabilities and synthetic tractability. Synthetic ease was not  
15  
16 only important with respect to medicinal chemistry, but also important when considering the WHO  
17  
18 recommendation that the cost of one antimalarial treatment is less than USD\$1.<sup>1</sup> Taking these criteria  
19  
20 into consideration, a survey of the HTS datasets identified the 2-anilino quinazoline as a promising  
21  
22 starting point.  
23  
24  
25  
26

27  
28 A sub-structure analysis across multiple screening data sets<sup>5-9</sup> revealed several analogues possessing  
29  
30 the 2-anilino quinazoline scaffold, with examples also included as part of the MMV Malaria Box.<sup>10</sup> A  
31  
32 summary of the number of hit analogues in each screening set and the activity of these analogues are  
33  
34 shown in Table S1. These analogues possess modest activity against asexual *P. falciparum* 3D7  
35  
36 parasites ( $EC_{50}$  ~0.1 to 2  $\mu$ M) and the multi-drug resistant parasite lines, K1, DD2 and W2 ( $EC_{50}$  ~0.1  
37  
38 to 2  $\mu$ M).<sup>7-9</sup> Further, this class has demonstrated modest activity against *P. falciparum* NF54 early  
39  
40 stage I-III gametocytes ( $EC_{50}$  ~1.5  $\mu$ M)<sup>5</sup> and examples that possessed *P. yoelii* liver stage schizonts  
41  
42 ( $EC_{50}$  ~0.1  $\mu$ M to 4  $\mu$ M),<sup>6</sup> while possessing a modest mammalian cell cytotoxicity window ( $EC_{50}$  >2  
43  
44  $\mu$ M).  
45  
46  
47  
48  
49

50  
51 Structurally related scaffolds have also been reported to possess antimalarial activity. A 2,4-  
52  
53 unsubstituted diaminoquinazoline scaffold was reported to target *Plasmodium* dihydrofolate reductase  
54  
55 (DHFR) and possess potent antimalarial activity (Figure 1).<sup>9, 11</sup> More recently, Chibale *et al.* have  
56  
57 described the optimization of the 2,4-diaminothienopyrimidine series<sup>12</sup> and Sambandamurthy *et al.* on  
58  
59  
60

1  
2 the development of a 2-aminopyridyl pyrimidine scaffold<sup>13</sup> that have yielded compounds with potent  
3  
4 antimalarial activity. Interestingly, the human methyl transferase inhibitor, BIX-01294, a 2,4-  
5  
6 substituted diaminoquinazoline was also found to be a potent antimalarial compound<sup>14</sup> (Figure 1). The  
7  
8 2-anilino quinazoline scaffold although structurally related to these other classes was sufficiently  
9  
10 structurally divergent to warrant further optimization. Only one other group 35 years ago has evaluated  
11  
12 the 2-anilino quinazoline scaffold for potential antimalarial activity.<sup>15</sup> In this study they show several  
13  
14 analogues possess varying degrees of efficacy in a *P. berghei* mouse model of disease burden, but did  
15  
16 not present any *in vitro* data or physicochemical data to facilitate optimization of this class, which we  
17  
18  
19  
20  
21 have now readdressed in the study undertaken here.<sup>16</sup>  
22  
23

24  
25 Herein, we describe the optimization of the 2-anilino quinazoline scaffold to generate a series of  
26  
27 compounds with potent activity primarily against the asexual stage of *P. falciparum*. Compounds with  
28  
29 these properties were then evaluated against *P. falciparum* gametocytes and multi-drug resistant strains,  
30  
31 and were further assessed in asexual stage growth arrest and rate of kill assays. Physicochemical  
32  
33 parameters were also assessed in parallel and assisted in the design and selection of analogues for  
34  
35 further evaluation in a mouse model of malaria disease burden.  
36  
37  
38

## 39 RESULTS AND DISCUSSION

40  
41  
42

43 The parasite activity of the analogues identified in the HT screening data sets, varied from one  
44  
45 research lab to another (Table S1). An attempt to build an early structure activity relationship (SAR)  
46  
47 proved challenging due to the variation in compound activity between data sets which was influenced  
48  
49 by different screening technologies, assay conditions and strain of parasite. Another challenge was that  
50  
51 the difference in functionality between analogues was highly varied and therefore difficult to  
52  
53 distinguish trends in early SAR. Thus, we initially sought to generate analogues in-house and acquire a  
54  
55 small set of closely related analogues to determine which functionality was important for activity  
56  
57  
58  
59  
60

1  
2 against *P. falciparum* asexual blood stages.<sup>17</sup> We then optimized the activity of these scaffolds  
3  
4 primarily based on *P. falciparum* asexual stage activity while monitoring mammalian cell cytotoxicity.  
5  
6

7  
8 To test the activity of compounds against asexual stage parasites, we utilized a *Plasmodium* lactate  
9  
10 dehydrogenase (pLDH) assay previously described.<sup>18</sup> Briefly, human erythrocytes infected with ring-  
11  
12 stage *P. falciparum* were treated with compounds or vehicle controls and incubated for 72 h. At the end  
13  
14 of this period, pLDH activity (monitored by the consumption of 3-acetylpyridine-adenine dinucleotide  
15  
16 (APADH), an NADH analogue) was determined as a measure of parasitemia. The human cellular  
17  
18 cytotoxicity of compounds was monitored by using a HepG2 growth inhibition assay using Cell Titre-  
19  
20 Glo.  
21  
22  
23

## 24 25 **Chemistry**

26  
27  
28 The synthetic route undertaken to generate the 2-anilino 4-substituted quinazolines involves two  
29  
30 generally high yielding S<sub>N</sub>Ar reactions using inexpensive building blocks (Scheme 1). The first S<sub>N</sub>Ar  
31  
32 reaction involves reaction of an amine that gives exclusively the 4-substituted regioisomer in moderate  
33  
34 to high yields across a range of different substrates. The second S<sub>N</sub>Ar reaction required the addition of  
35  
36 a strong acid to adequately activate the 2-position of the quinazoline for nucleophilic addition by the  
37  
38 aniline. Using these conditions and microwave irradiation the 2-anilino substituted products were  
39  
40 obtained in acceptable yields.  
41  
42  
43  
44  
45

## 46 **Structure and activity relationship**

47  
48  
49 We first investigated whether the substitution at the 4-position was important for activity, while  
50  
51 retaining an aniline substituent in the 2-position. It was observed (Table 1) that disubstitution of the 4-  
52  
53 nitrogen (examples **2**, **3**, and **8**) was detrimental to activity (7.6 μM, 1.8 μM and 418 nM respectively)  
54  
55 compared to the mono-alkyl amino compounds **1** (124 nM) and **4** (329 nM). However, the compound  
56  
57  
58  
59  
60

1  
2 possessing an N-methyl substituent at the 4-position (analogue **7**) had comparable activity (124 nM) to  
3  
4 analogue **3** with a larger N-(3-hydroxypropyl) substituent. This data suggested that the 4-NH group was  
5  
6 required for binding to its cellular target, and that substitution on the 4-amino group is likely oriented  
7  
8 towards solvent space. A number of screening hits (as seen in Table S1) possessed either a  
9  
10 furfurylamino or tetrahydrofurfurylamino group in the 4-position. To investigate whether these groups  
11  
12 in the 4-position were important for activity, several analogues were generated with this functionality.  
13  
14 As a general observation, these groups had no effect on activity (Table 1), and therefore could be used  
15  
16 interchangeably for SAR purposes.  
17  
18  
19

20  
21 We next investigated the effect of substitution on the 2-aniline moiety on the activity against  
22  
23 erythrocytic stage parasites, while maintaining either the furfurylamino and tetrahydrofurfurylamino  
24  
25 groups in the 4-position. It was shown that the *meta*-methoxy compound **23** and related *para*-methoxy  
26  
27 compound **1** both possessed EC<sub>50</sub> values of 230 nM and 124 nM respectively, however the *ortho*-  
28  
29 methoxy analogue **24** possessed reduced activity (526 nM) (Table 1). This was further exemplified  
30  
31 with *ortho*-substituted dimethoxy analogues **25** and **26**, which were observed to have weaker activity  
32  
33 (1.6 and 1.3 μM) compared to the 3,4-methylenedioxy analogues **22** and **5** (169 and 114 nM  
34  
35 respectively). Larger polar substituents in the 4-position, such as an ester (**17**), 1-hydroxyethyl (**18**),  
36  
37 amide (**19** and **20**), or an acetamide (**21**) were not well tolerated (574, 702, 691, 569, and 274 nM  
38  
39 respectively) compared to **1** (124 nM).  
40  
41  
42  
43  
44  
45

46  
47 We noted that the methoxy analogues carried potential metabolic liabilities particularly in the 4-  
48  
49 position of the aniline. Metabolism studies (Table S2) identified that the 4-methoxy substituent on the  
50  
51 aniline is O-demethylated and subsequently oxidized to the quinone functionality that is potentially  
52  
53 susceptible to the addition of nucleophiles and a site for glucuronidation. To address this liability, we  
54  
55 then replaced the 4-methoxy substituent with methyl and halogen substituents. It was observed that the  
56  
57 4-halogen analogues **10-12** (125, 112, and 113 nM respectively) and the 4-methyl analogue **9** (109 nM)  
58  
59  
60

1  
2 all retained potency compared to the 4-methoxy analogue **1** (124 nM) (Table 1). Notably, the 4-halogen  
3 analogues also maintained a selectivity window of approximately 50-fold or greater with a slightly  
4 better selectivity profile to the methoxy analogues **1** and **23**. Consistent with the decrease in activity of  
5 other *ortho*- substituted 2-anilino analogues, the *ortho*-fluoroaniline (**16**) also had decreased  
6 antimalarial activity (317 nM). However, analogues with either *meta*-chloro or *meta*-fluoro substitution  
7 on the aniline (**14** and **15** respectively) exhibited activity (134 and 144 nM) comparable to the *para*-  
8 fluoro analogue **12** (112 nM).  
9  
10  
11  
12  
13  
14  
15  
16  
17

18  
19 The furfurylamino and tetrahydrofurfurylamino groups present in many of the screening hits (Table S1)  
20 and compounds detailed in Table 1, have been previously identified as liabilities in liver microsome  
21 studies.<sup>19, 20</sup> The identification of metabolites from liver microsome studies corroborated this  
22 observation (Table S2). In the first instance, to block this metabolic liability the 4-furfurylamino and 4-  
23 tetrahydrofurfurylamino groups were replaced with a 4-benzylamino group. The activity (77 and 264  
24 nM) of 4-benzylamino analogues **29** and **27** with either 4-methoxy or 4-fluoro substitution on the 2-  
25 anilino moiety (Table 2) demonstrated that the benzyl group was tolerated compared to their furfuryl  
26 counterparts, **1** and **12** (124 and 112 nM). Furthermore, it suggested that the 4-position could be used as  
27 a site at which to attach functionalities that could improve the overall physicochemical properties of the  
28 scaffold, given that physicochemical analysis revealed that **27** possesses high cLogP (Table 2) and  
29 limited aqueous solubility (Table 5).  
30  
31  
32  
33  
34  
35  
36  
37  
38  
39  
40  
41  
42  
43  
44  
45

46 The incorporation of the 4-halogen substitution on the aniline prevented O-demethylation, but  
47 presented its own metabolic liability.<sup>21</sup> Metabolism identification studies revealed that the 4-halogen  
48 substituent (analogues **36** and **35**) was susceptible to hydro-dehalogenation (Table S2). A known  
49 method in literature to suppress hydro-dehalogenation from occurring is to incorporate a 3-halogen  
50 substituent next to the 4-halogen.<sup>22</sup> Several analogues **31-33** with 3,4-dihalogen substitution were  
51 generated and possessed similar antimalarial activity (56 to 121 nM) compared to the 4-fluoro analogue  
52  
53  
54  
55  
56  
57  
58  
59  
60

1  
2 77 (77 nM) (Table 2). Notably, the 3-chloro-4-fluoro analogue **32** was similarly potent (56 nM) to other  
3  
4 di-halogen analogues **31** and **33** (98 and 121 nM respectively). It was also observed that replacing the  
5  
6 aniline with 4-trifluoromethyl pyridin-3-yl amine (**34**) retained activity (102 nM) compared to the  
7  
8 trifluoromethylaniline orthologue **30** (105 nM). This results suggests that the aniline moiety can be  
9  
10 replaced with a pyridine and provides a future opportunity to overcome metabolism issues and adverse  
11  
12 toxicity of reactive metabolites associated with anilines. Data from the metabolite study undertaken on  
13  
14 compounds **53-56** (see below) corroborated that hydro-dehalogenation was suppressed by the 3,4-  
15  
16 dihalogen substitution. However, inserting a benzyl group in the 4-position and substituting halogens  
17  
18 on the 2-aniline (compounds **29-33**) to improve metabolism, impacted cLogP and in turn LipE values  
19  
20 were unsatisfactorily low (Table 2).  
21  
22  
23  
24  
25

26  
27 To improve the LipE, solubility, and target selectivity of the series, we then incorporated a heteroatom  
28  
29 replacement into the 5, 7 or 8 positions of the quinazoline ring, and also replaced the quinazoline  
30  
31 system with similar heteroaromatic systems. Several analogues **37-42** were synthesized to evaluate  
32  
33 whether these changes would be tolerated with respect to asexual antimalarial activity. Analogues **37**,  
34  
35 **38**, **40-42** in this assay showed reduced potency (539 nM, 636 nM, 866 nM, 1.3  $\mu$ M and 7.7  $\mu$ M  
36  
37 respectively) compared to the comparator compound **29** (77 nM) (Table 3). Compound **39** was the  
38  
39 exception, possessing similar activity (57 nM) to **29** (77 nM). Compound **39** can form an  
40  
41 intramolecular hydrogen bond between the 5-heteoatom and the 4-NH group, potentially masking the  
42  
43 4-NH from its binding partner and affecting the intrinsic lipophilicity. However, methylation of the 4-N  
44  
45 position reduces antimalarial activity, and therefore it is unclear whether the intramolecular hydrogen  
46  
47 bond contributes to biological activity. Nevertheless, the pyridyl scaffold present in compound **39**  
48  
49 offered an avenue to improve LipE and thus was further utilized later in the optimisation of the series.  
50  
51  
52  
53  
54  
55

56 6,7-Dimethoxy analogues **35** and **36** were also prepared to improve LipE, and this substitution  
57  
58 preserved activity (57 and 41 nM respectively) (Table 3) compared to **29** (77 nM) (Table 2). However,  
59  
60

1  
2 O-demethylation of both 6 and 7 methoxy groups was shown to be responsible for high intrinsic  
3 clearance in liver microsome studies (Table S2). Therefore, this substitution was not pursued further.  
4  
5  
6

7  
8 In an ongoing effort to improve physicochemical properties of the series we next looked at replacing  
9 the hydrophobic aliphatic substitution in the 4-position with polar substituents. This change was  
10 orchestrated to more specifically reduce cLogP and improve solubility. From earlier SAR (Figure 2), it  
11 was evident that the substitution in the 4-position was not important for modulating antimalarial  
12 activity, suggesting that this moiety of the molecule not involved in binding to its cellular target, but  
13 instead oriented towards solvent space. This provided an avenue to install groups known to assist in  
14 improving solubility. To test this hypothesis, we generated several analogues **47-52** with polar  
15 functionality in the 4-position while retaining the 4-fluoroaniline in the 2-position and evaluated their  
16 asexual antimalarial activity (Table 4). Compared to **29** (77 nM), **47**, **49** and **50** had similar activity  
17 (104, 118 and 77 nM), while **48**, **51** and **52** had a marginal improvement in activity (42, 64 and 51 nM).  
18 Notably, **47-52** had an improved selectivity window of 250-fold or greater and improved LipE  
19 compared to the progenitor compound **29**.  
20  
21  
22  
23  
24  
25  
26  
27  
28  
29  
30  
31  
32  
33  
34  
35  
36

37 We then combined the functionality from the 2 and 4 positions that best modulated antimalarial  
38 potency to generate analogues **53-56** that had a combination of 2-(4-methylpiperazin-1-yl)-ethylamino  
39 or 4-amino-1-methylpiperidinyl groups in the 4-position and either 4-chloro-3-fluoroanilino or 3-  
40 chloro-4-fluoroanilino groups in the 2-position of the quinazoline (Table 4). The same substitution  
41 patterns were also installed on the most promising heteroaryl quinazoline system, pyrido[3,2-  
42 d]pyrimidine (derived from compound **29**), to generate analogues **43-46** (Table 4). The evaluation of  
43 these compounds, **43-46** and **53-56**, against the asexual stage of *P. falciparum* parasites showed that the  
44 pyrido[3,2-d]pyrimidine analogues (**43-46**) all possessed EC<sub>50</sub> values greater than 110 nM (Table 4).  
45 The non-heteroaromatic derivatives **53-56** were more potent with EC<sub>50</sub> values ranging from 25 to 35  
46 nM. The 2-(4-methylpiperazin-1-yl)-ethylamino analogues **53** and **54** had a selectivity window of  
47  
48  
49  
50  
51  
52  
53  
54  
55  
56  
57  
58  
59  
60

1  
2 ~250-fold, whereas the 4-amino-1-methylpiperidinyl analogues **55** and **56** ~150-fold (Table 4). Given  
3  
4 that **53-56** possessed the most potent activity against *P. falciparum* parasites *in vitro*, we further  
5  
6 assessed the physicochemical properties and parasite activity of these analogues.  
7  
8

9  
10 The solubility of analogues **53-56** at both pH 2 and pH 6.5, as measured by nephelometry, was  
11  
12 enhanced compared to compounds that did not possess 2-(4-methylpiperazin-1-yl)-ethylamino or 4-  
13  
14 amino-1-methylpiperidinyl functionality in the 4-position (Table 5). The stability of **53-56** in the  
15  
16 presence of both human liver and mouse microsomes was also enhanced as shown by the improvement  
17  
18 in the hepatic extraction ratio and predicted intrinsic clearance values compared to the earlier analogue  
19  
20 **27** (Table 5). Notably, an across species difference in the liver microsome study was observed, where  
21  
22 compounds were generally more susceptible to degradation in the presence of mouse liver microsomes  
23  
24 than human. Interestingly, the 4-amino-1-methylpiperidinyl **55** and **56** were more stable than their 2-  
25  
26 (4-methylpiperazin-1-yl)-ethylamino counterparts **53** and **54** in the presence of mouse liver  
27  
28 microsomes.  
29  
30  
31  
32

33  
34 The major metabolites identified in the microsome studies for analogues **53-56** were N-demethylation  
35  
36 of the methylpiperidine or piperazine, and mono-oxygenation, presumably at the 6-position of the  
37  
38 quinazoline (Table S2). In these studies, a minor metabolite with a mass consistent with hydro  
39  
40 defluorination was also observed for the 3-chloro-4-fluoro anilino analogues **53** and **55**. It is known that  
41  
42 a 4-fluorine substituent is more susceptible to hydro dehalogenation than a 4-chloro,<sup>23</sup> which is  
43  
44 consistent with the differences observed in this metabolism study between **53/55** and **54/56**.  
45  
46 Nevertheless, the hydro defluorination was suppressed in the cases of the dihalo analogues **53-56**  
47  
48 compared to that of mono-fluoro analogue **36** (Table S2). It is currently not known whether the  
49  
50 metabolites of compounds **53-56** possess antimalarial activity, so blocking these sites of metabolism  
51  
52 may not be beneficial for *in vivo* antimalarial activity. The blood plasma concentrations of the  
53  
54 metabolites are also unknown, and therefore will be investigated in the future development of the 2-  
55  
56  
57  
58  
59  
60

1  
2 anilino quinazoline series. Further efforts to block these metabolic events and improve on the  
3  
4 physicochemistry of the series, particularly concentrating LipE, will be the focus of future  
5  
6 optimization.  
7

### 8 9 10 **Evaluation against a multi-drug resistant strain of *P. falciparum***

11  
12  
13 Several hit compounds from previous studies have been shown to be effective against different drug-  
14 resistant strains of *P. falciparum*<sup>7-9</sup> (Table S1). We evaluated a selection of compounds from our series  
15  
16 against the chloroquine and mefloquine resistant W2mef strain of *P. falciparum* using the LDH assay  
17  
18 format described above. This strain expresses a mutant PfCRT that confers chloroquine resistance, as  
19  
20 well as amplified levels of the digestive vacuole drug transport channel, P-glycoprotein homologue 1  
21  
22 (Pgh1), encoded by the *pfmdrl* gene that confers resistance to mefloquine.<sup>24</sup> From the data presented in  
23  
24 Table 6, W2mef parasites showed sensitivity towards the selected compounds that were similar to the  
25  
26 chloroquine- and mefloquine-sensitive 3D7 parasite strain. Notably, compounds **53-56**, that harbor  
27  
28 basic functionality with pKa values similar to the functionality found on mefloquine and chloroquine,  
29  
30 were active against the W2mef line, suggesting they are not substrates of PfCRT or the Pgh1 drug  
31  
32 transport channel.  
33  
34  
35  
36  
37  
38  
39

### 40 **Determination of the rate of kill and the stage of arrest in asexual stage *P. falciparum* parasites**

41  
42  
43 To align the 2-anilino quinazoline series with target product profile criteria suggested by world  
44 health governing bodies,<sup>1</sup> it is important to define the stage at which these compounds impact asexual  
45  
46 lifecycle progression, and also the rate at which this series arrests *P. falciparum* parasites *in vitro*  
47  
48 (Figure 3 and Figure 4). To determine the stage of arrest, synchronous ring (>95%) or trophozoite stage  
49  
50 3D7 parasites (>90%), were treated with compound at a concentration 10 times their EC<sub>50</sub>. At 0, 24 and  
51  
52 48 h, blood smears were prepared with Giemsa staining and the morphology and parasite form was  
53  
54 quantified. The data from this study is summarized in Figure 3 and shows that four compounds, namely  
55  
56  
57  
58  
59  
60

1  
2 **53-56**, generally arrest the majority of parasites at the ring stage of asexual stage development,  
3  
4 commonly leading to parasite death. It was also observed that when compared to DMSO-treated  
5  
6 controls, treatment with any one of compounds **53-56** at the ring stage, only one third of parasites  
7  
8 progressed to the trophozoite stage, and virtually none completed schizogony or advanced into the next  
9  
10 cell cycle. Conversely, a proportion of parasites that were treated with one of **53-56** at the trophozoite  
11  
12 stage were able to complete schizogony and enter the next lifecycle, but were then arrested at the next  
13  
14 ring stage. It is interesting to note that compounds **53-56** behave similarly to artemisinin, the current  
15  
16 gold standard antimalarial treatment, in that they also arrest parasite growth at the ring stage of the  
17  
18 parasite's asexual lifecycle<sup>25</sup> (Figure 3).  
19  
20  
21  
22  
23

24 We next performed a compound washout experiment to confirm the stage of asexual arrest and rate of  
25  
26 action of **53** and **54**, as **55** and **56** performed so similarly in the stage arrest experiments. In this study,  
27  
28 synchronous *P. falciparum* 3D7 ring stage parasites expressing nanoluciferase<sup>26</sup> were treated with a  
29  
30 dilution series of the compound (maximum concentration 500 times the EC<sub>50</sub>) at time point 0, and then  
31  
32 the compound was washed out at 3, 6 and 24 h time points (Figure 4). All parasites were allowed to  
33  
34 grow for a total of 24 h and the parasite viability was subsequently quantified by measuring  
35  
36 bioluminescence. EC<sub>50</sub> values were then calculated for each pulse point. The data presented in Figure 4  
37  
38 demonstrates that the EC<sub>50</sub> for **53** and **54** gradually declines after 6 h suggesting the compounds  
39  
40 progressively arrest parasite growth over 24 h in a concentration dependent manner. The fact the drugs  
41  
42 reduce ring-stage growth over the first several hours of treatment supports the findings in Figure 3.  
43  
44 Chloroquine acted over a similar timeframe, but chloroquine was significantly more potent at the  
45  
46 timepoints measured than **53** and **54**. Whereas artemisinin appears to maximally reduce parasite growth  
47  
48 between 3 h and 6 h,<sup>25</sup> indicating that it acts more quickly and at lower concentrations than **53** and **54**.  
49  
50  
51  
52  
53  
54  
55

56 **Lead compound evaluation against sexual stage *P. falciparum* gametocytes**  
57  
58  
59  
60

1  
2 In the sexual stage of the parasites lifecycle, a small number of the asexual forms commit to the  
3 sexual development of the parasite through a process termed gametocytogenesis. After commitment,  
4 which occurs over a single inter-erythrocytic replication cycle, ring stage parasites are present which  
5 although not distinguishable from asexual blood stage parasites initially, continue through a  
6 developmental differentiation pathway through five morphological recognizable stages (I to V)  
7 ultimately culminating in the presence of both male and female gametocytes that can be transmitted  
8 from the blood of the host to the mosquito during a blood meal. The ability for an antimalarial agent to  
9 block transmission of the malaria parasite from the human host to the mosquito is critical in the  
10 worldwide effort to prevent malaria transmission. World governing bodies and MMV have suggested  
11 several target product profiles that encompass agents that kill gametocytes and could potentially act as  
12 transmission blocking agents.  
13  
14  
15  
16  
17  
18  
19  
20  
21  
22  
23  
24  
25  
26  
27  
28

29 To determine if the lead compounds **53-56** from the 2-anilino quinazoline series were suitable to fit  
30 this profile, these compounds were evaluated for their ability to prevent gametocyte development and  
31 reduce viability at three stages of gametocyte development, ring stage, early stage (I-III) or late stage  
32 (IV-V). A previously described high content imaging assay using a highly synchronous culture of *P.*  
33 *falciparum* NF54<sup>pfs16-LUC-GFP</sup> parasites that have been treated with N-acetyl glucosamine at day 0 of  
34 gametocyte development to prevent asexual growth and replication was employed.<sup>5</sup> Compound effects  
35 on gametocyte development and viability after 72 h incubation were determined using automated  
36 image analysis of confocal microscopic images whereby GFP was used to define gametocyte  
37 morphology and MitoTracker Red (MTR CM-H2XRos) was used to define parasite viability.  
38  
39  
40  
41  
42  
43  
44  
45  
46  
47  
48  
49  
50

51 The results of this study demonstrate that compounds **53-56** are most potent against ring stage  
52 gametocytes (179 - 223 nM), and less so against early stage gametocytes (326 - 554 nM) and weakly  
53 active against late stage gametocytes (>2  $\mu$ M) (Table 7). A comparison of this data with the asexual  
54 stage data shows that parasites arrest at both the early stages of asexual and sexual stage development.  
55  
56  
57  
58  
59  
60

1  
2 These compounds are also 10-fold less potent against ring stage gametocytes and 15 to 25-fold less  
3  
4 potent against early stage gametocytes compared with activity against early asexual stage parasites (26  
5  
6 - 35 nM). Some reasons postulated for this difference are that the cellular target(s) of **53-56** are not  
7  
8 expressed or are not as essential for gametocytogenesis as they are for the asexual blood stage. Another  
9  
10 hypothesis is that **53-56** acts on two or more cellular targets essential for asexual stage progression, but  
11  
12 only have modest affinity for a target(s) that is only expressed during gametocyte development. To find  
13  
14 a more definitive reason for these differences in stage specific potency, we are now attempting to  
15  
16 identify the cellular target of the 2-anilino quinazoline series.  
17  
18  
19

### 20 21 22 **Evaluation of compounds in a mouse model of malaria disease burden** 23

24  
25 Overall the physical properties installed in analogues **53-56**, along with their potent asexual  
26  
27 antimalarial activity, suggested they were suitably placed for evaluation in a mouse model of malaria  
28  
29 disease burden. A Peters 4 day mouse model was employed to determine the primary *in vivo*  
30  
31 antimalarial activity of compounds **53-56**.<sup>27</sup> In this model, mice were infected with *P. berghei* ANKA  
32  
33 parasites on day 0. Compounds were then administered either by intraperitoneal injection (i.p.) or oral  
34  
35 gavage (p.o.) at 20 mg/kg, 4 hours after infection and then on day 1, 2 and 3. On the fourth day blood  
36  
37 smears were taken and parasitemia evaluated. A summary of these studies is shown in Figure 5 (panels  
38  
39 A and B).  
40  
41  
42  
43  
44

45 The mouse blood plasma exposure levels of compounds **53-56** in this mouse model were also  
46  
47 monitored at 2, 5 and 20 h after administration of treatment at day 0. The results for each compound  
48  
49 **53-56** are shown in Figure 5 (panels C and D) and Table S3. The blood plasma exposure levels  
50  
51 observed with compounds **53-56** in this model by either i.p. or p.o administration over 20 h were  
52  
53 significantly higher than the concentrations required to suppress parasite growth *in vitro*, consistent  
54  
55 with the *in vivo* efficacy observed.  
56  
57  
58  
59  
60

1  
2 In the Peter's 4-day mouse model, compounds that possess a 4-amino ethyl piperazine substituent,  
3  
4 **53** and **54**, reduced parasitemia by >98% when administered intraperitoneally (Figure 5A) and by  
5  
6 >90% when administered orally (Figure 5B). Compounds **53** and **54** reduced parasitemia to a similar  
7  
8 extent, even though **53** had a greater blood plasma exposure than **54** when dosing either by i.p. or p.o.  
9  
10 The mean levels of parasitemia in mice treated intraperitoneally with compounds that possess the 4-  
11  
12 amino piperidine, **55** and **56**, were higher than **53** and **54** (Figure 5A). A likely explanation for this  
13  
14 trend is that compounds **55** and **56** had lower blood plasma exposure levels in comparison to **53** and **54**  
15  
16 (Figure 5C). When dosed by oral gavage, compound **55** reduced parasitemia to similar levels to **53** and  
17  
18 **54**, in contrast the mean parasitemia value for compound **56** was higher (Figure 5B). Reflecting this  
19  
20 result, compound **56** demonstrated the lowest blood plasma exposure level in comparison to  
21  
22 compounds **53-55** (Figure 5D). In summary of the mouse model, the structural differences versus the  
23  
24 performance between compounds **53-56** could not be definitively concluded (dosing either i.p. or p.o.)  
25  
26 because the statistical test between compounds was not significant. However, the data between the  
27  
28 vehicle control and compounds **53-56**, was statistically significant. Collectively this preliminary *in vivo*  
29  
30 data shows that the lead compounds in the anilino quinazoline series are orally efficacious, but require  
31  
32 further optimization for complete suppression of parasitemia at lower doses of compound.  
33  
34  
35  
36  
37  
38  
39  
40  
41  
42  
43

## 44 CONCLUSIONS

45  
46  
47 In this report, we have described the optimization of the 2-anilino quinazoline series to generate lead  
48  
49 compounds that have potent antimalarial activity against asexual stage parasites. Furthermore, these  
50  
51 compounds are shown here to have comparable *in vitro* activity to chloroquine and mefloquine. The 2-  
52  
53 anilino quinazoline series also has a similar activity profile against the W2mef multi-drug resistant  
54  
55 parasite line compared to 3D7 *P. falciparum* parasites. The lead compounds, however, are 10-fold  
56  
57  
58  
59  
60

1  
2 weaker against ring stage gametocytes, and less potent against early stage and late stage gametocytes.  
3  
4 The 2-anilino quinazoline series was shown to be moderately fast acting and exerts its greatest effect at  
5  
6 the ring phase in the asexual stage and at ring stage of gametocytogenesis.  
7  
8

9  
10 The remaining challenges for the next phase of optimization of this series will include monitoring of  
11  
12 cardiotoxicity risk (hERG) and other mammalian targets that are commonly associated with adverse  
13  
14 safety risks; particularly given the lipophilicity and basic functionality the series currently possesses  
15  
16 and that this scaffold is often considered as promiscuous. To identify potential off-target promiscuity, a  
17  
18 sub-structure search of literature was performed and revealed several compound series that possess the  
19  
20 4-amino 2-anilinoquinazoline substructure that inhibit, with varying potencies, human kinases,<sup>28-30</sup>  
21  
22 ATPases<sup>31-33</sup> and G-protein coupled receptors.<sup>34-36</sup> As a consequence, off-target activity, particularly  
23  
24 those associated with safety risks, will be monitored in the future development of this compound class.  
25  
26  
27  
28  
29

30 The potential metabolic liability and toxicity associated with the 2-aniline moiety also needs to be  
31  
32 addressed. It is foreseen that this liability will likely be tackled by replacing the 2-anilino group with  
33  
34 pyridyl functionality, given that the 2-pyridyl analogue **34** was shown to have equivalent potency and  
35  
36 improved cLogP compared to the parent 2-aniline compound **30**. Improving the LipE of the series is  
37  
38 also a priority. Inserting heteroatoms into the scaffold, such as that seen in **34**, along with substituting  
39  
40 different polar aliphatic functionality in the 4-position, as seen in **51**, is an obvious avenue to improve  
41  
42 LipE in further development of the 2-anilino quinazoline series. Although the physicochemical  
43  
44 properties, namely solubility and metabolism, of the lead compounds **53** and **54**, are superior to the  
45  
46 screening starting points, additional effort is required to optimize these properties.  
47  
48  
49  
50  
51

52 In closing, we have optimized a set of publicly available screening hits to compounds that are able to  
53  
54 arrest the growth and development of asexual stage parasites, with comparable activity to chloroquine,  
55  
56 and can suppress 99.8% and 95% of parasitemia in a mouse model when dosed at 20 mg/kg  
57  
58  
59  
60

1  
2 intraperitoneally and orally and respectively. It is foreseen that with further optimization, this  
3  
4 chemotype will join the current arsenal of new agents progressing towards and through the clinic to  
5  
6 assist in treating and eliminating this devastating disease.  
7  
8  
9

## 10 11 12 13 14 15 **EXPERIMENTAL SECTION**

16  
17 **Asexual Stage Parasite Viability Assay.** *P. falciparum* 3D7 and W2mef parasites were cultured  
18  
19 according to the procedure described by Jensen *et al.*<sup>37</sup> in RPMI-HEPES media supplemented with L-  
20  
21 glutamine and Albumax II. 100  $\mu$ L of *P. falciparum* ring-stage cultures were seeded into 96-well  
22  
23 microplates at 0.3% parasitemia and 2% hematocrit. Compounds were serially diluted in DMSO at the  
24  
25 appropriate working concentration and were added to cultures with a final concentration of 0.2%  
26  
27 DMSO. The growth assays were performed in triplicate for 1.5 cell cycles (37°C, 72 h). The cultures  
28  
29 were then lysed by a freeze-thaw cycle and 30  $\mu$ L was mixed with 75  $\mu$ L of modified Malstat reagent<sup>18</sup>  
30  
31 (0.1 M Tris pH 8.5, 0.2 g/mL lactic acid, 0.2% v/v Triton X-100 and 1 mg/mL acetylpyridine adenine  
32  
33 dinucleotide), 0.01 mg/mL phenazine ethosulfate and 0.2 mg/mL nitro blue tetrazolium. Once the no  
34  
35 drug control wells had developed a purple color the absorbance was measured at 650 nm in a  
36  
37 spectrophotometer. Absorbance values were plotted using a 4 parameter log dose, non-linear regression  
38  
39 analysis, with sigmoidal dose response (variable slope) curve fit in GraphPad Prism (ver 6.05) and  
40  
41 normalized against untreated and uninfected samples to generate drug curves and EC<sub>50</sub> values.  
42  
43 Chloroquine (EC<sub>50</sub> of 23 nM for 3D7 and an EC<sub>50</sub> of 250 nM for W2mef) and Artemisinin (EC<sub>50</sub> of 8  
44  
45 nM for 3D7 and an EC<sub>50</sub> of 6 nM for W2mef) were used as control compounds.  
46  
47  
48  
49  
50  
51  
52  
53  
54

55 **HepG2 Viability Assay.** HepG2 cells were cultured in Dulbeccos modified eagles medium (DMEM)  
56  
57 supplemented with 10% fetal calf serum (FCS), in a humidified incubator at 37°C and 5% CO<sub>2</sub>. Ten  
58  
59  
60

1  
2 point compound titration assays were performed by treating cells ( $1 \times 10^3$ ) for 48 h in 384 well tissue  
3 culture treated plates (Greiner). Cytotoxicity was determined using Cell Titer Glo (Promega) and  
4 calculated as a percentage using DMSO as a positive growth control and 10  $\mu\text{M}$  Bortezomib as a  
5 negative growth control.  $\text{EC}_{50}$  values were calculated using a 4 parameter log dose, non-linear  
6 regression analysis, with sigmoidal dose response (variable slope) curve fit using Graph Pad Prism (ver  
7 6.05). 0 and 100 constraint parameters were used for curve fitting. Etoposide was used as a control  
8 compound and was determined to have an  $\text{EC}_{50}$  of 15.9  $\mu\text{M}$ , compared to the literature value  $\text{EC}_{50}$  of  
9 30.2  $\mu\text{M}$  that had an incubation time of 48 h using an MTT assay to determine cell viability.<sup>38</sup> For a  
10 comparison, the following known antimalarials were evaluated in the HepG2 viability assay;  
11 chloroquine  $\text{EC}_{50} >40 \mu\text{M}$ ; artemisinin  $\text{EC}_{50} >40 \mu\text{M}$ ; atovaquone  $\text{EC}_{50} 23.2 \mu\text{M}$ ; mefloquine  $\text{EC}_{50}$   
12 11.6  $\mu\text{M}$ .  
13  
14  
15  
16  
17  
18  
19  
20  
21  
22  
23  
24  
25  
26  
27  
28  
29  
30

31 **Rate and Stage of Asexual Parasite Arrest Study.** 3D7 parasites  $\pm$  nanoluciferase<sup>26</sup> were  
32 maintained as synchronized cultures by frequent sorbitol treatment of ring stages. Prior to commencing  
33 experiments, Giemsa-stained smears the parasites were counted to ensure the stage required was over  
34 90% pure. To determine stage of arrest, following synchronization (rings) or 24 h later (trophozoites),  
35 parasites were treated with 10 times  $\text{EC}_{50}$  of each compound. Parasites were smeared immediately prior  
36 to addition of compound (time point 0) and again after 24 and 48 h and subsequently fixed in methanol  
37 (30 sec) and stained by incubation with 10% Giemsa solution (5 min). 1000 cells were counted per  
38 treatment, per time point for three independent biological replicates.  
39  
40  
41  
42  
43  
44  
45  
46  
47  
48  
49

50 To determine the rate of parasite arrest, sorbitol synchronized parasites were diluted to 1%  
51 hematocrit and 100  $\mu\text{L}$  was added to the wells of a 96-well plate. Compounds were added in a two-fold  
52 dilution series in DMSO with the highest concentration being 500 times the  $\text{EC}_{50}$  of each compound  
53 and final DMSO concentration at 0.2%. After specific periods of drug incubation (3, 6 or 24 h), treated  
54  
55  
56  
57  
58  
59  
60

1  
2 cells were washed four times by removing 80  $\mu\text{L}$  of media and replacing it with 200  $\mu\text{L}$  fresh media.  
3  
4 Following washing, parasites were incubated at 37°C for the remainder of the 24 h growth period. To  
5  
6 measure parasite viability, parasites were re-suspended and 10  $\mu\text{L}$  of each well was added to a 96-well  
7  
8 Costar luminescence plate. Cells were subsequently lysed by addition of 90  $\mu\text{L}$  lysis buffer (10 mM tris  
9  
10 phosphoric acid, 5 mM  $\text{K}_2\text{EDTA}$ , 0.2% NP40, 5 mM DTT). To measure bioluminescence, 5  $\mu\text{L}$  of  
11  
12 NanoGlo-containing buffer (20  $\mu\text{L}$  NanoGlo substrate per ml of buffer (10 mM tris phosphoric acid,  
13  
14 132 mM NaCl, 5 mM  $\text{K}_2\text{EDTA}$ , 5 mM DTT, 0.5 mM Tris-HCl, pH 7.5)) was injected into each well,  
15  
16 prior to shaking (700 pm/30 sec). Relative light units were measured with a CIARIOstar multimode  
17  
18 plate reader (BMG Labtech) and data was subsequently analyzed using GraphPad PRISM software.  
19  
20  
21  
22  
23  
24

25  
26 **Sexual Stage High Content Imaging Assay.** Sexual stage activity of compounds was evaluated  
27  
28 according to the method of Duffy *et al.*<sup>5</sup> Briefly, NF54<sup>pfs16-LUC-GFP</sup> transgenic parasites expressing GFP  
29  
30 linked to luciferase under the control of the early gametocyte specific pfs16 promoter, Pfs16 were  
31  
32 maintained in asexual culture. At day -3 and -2 of the induction of gametocytogenesis, magnet purified  
33  
34 trophozoites were placed under nutritional stress in order to induce gametocytogenesis.<sup>39</sup> At day 0 of  
35  
36 gametocyte development, N-acetyl glucosamine (NAG) (50 mM) was added to the parasite culture to  
37  
38 prevent asexual parasite replication. Gametocytes were then obtained after continuous culture at the  
39  
40 appropriate time points, ring stage (day 0), early stage (day 2) and late stage (day 8).<sup>39</sup> Titrated  
41  
42 compound diluted in 4% DMSO was transferred into 384-well imaging plates. The independent  
43  
44 gametocyte cultures at the appropriate stage were dispensed into the compound containing imaging  
45  
46 plates which were then sealed and incubated for 72 h in standard incubation conditions of 5%  $\text{CO}_2$ , 5%  
47  
48  $\text{O}_2$  and 60% humidity at 37°C. After 72 h incubation, 5  $\mu\text{L}$  of MitoTracker Red CMH2XRos (MTR) in  
49  
50 phosphate buffered saline (PBS) was added to each well and plates were resealed with membranes and  
51  
52 incubated overnight. The following day image acquisition and analysis was undertaken on the Opera  
53  
54 QEHS micro-plate confocal imaging system. Single images were taken for each well and the GFP  
55  
56  
57  
58  
59  
60

1  
2 intensity was measured with an exposure time of 400 msec (488 nm), then to ascertain the fluorescence  
3  
4 intensity of the viability stain, MTR, measurements were made for 600 msec (532 nm). All images, for  
5  
6 each well, were analyzed using an Acapella based script which relates the MTR fluorescent signal and  
7  
8 the GFP designated object quantifying viable stage dependent parasite morphology. Gametocyte  
9  
10 viability after a 72 h incubation was calculated as a percentage of the positive (5  $\mu$ M puromycin) and  
11  
12 negative (0.4% DMSO) controls contained in each assay plate.  $EC_{50}$  values were calculated using a 4  
13  
14 parameter log dose, non-linear regression analysis, with sigmoidal dose response (variable slope) curve  
15  
16 fit using GraphPad Prism (ver 4.0). No constraints were used in the curve fit. Chloroquine, Artesunate,  
17  
18 Pyronaridine were used as control compounds and their  $EC_{50}$  values are indicated in Table 7 and are  
19  
20 directly comparable to  $EC_{50}$  values cited in Duffy *et al.*<sup>5</sup>  
21  
22  
23  
24  
25  
26  
27

28 **Solubility Determination using Nephelometry.** Compound in DMSO was spiked into either pH  
29  
30 6.5 phosphate buffer or 0.01 M HCl (approx pH 2.0) with the final DMSO concentration being 1%.  
31  
32 Samples were then analyzed via nephelometry to determine a solubility range.<sup>40</sup>  
33  
34  
35  
36

37 ***In Vitro* Metabolism using Mouse and Human Liver Microsomes.** Metabolic stability was  
38  
39 assessed by incubating test compounds individually (1  $\mu$ M) at 37°C with either mouse or human liver  
40  
41 microsomes. The metabolic reaction was initiated by the addition of an NADPH regenerating system  
42  
43 and quenched at various time points over the incubation period by the addition of acetonitrile. The  
44  
45 relative loss of parent compound and formation of metabolic products was monitored by LC-MS. Test  
46  
47 compound concentration versus time data was fitted to an exponential decay function to determine the  
48  
49 first-order rate constant for substrate depletion. In cases where clear deviation from first-order kinetics  
50  
51 was evident, only the initial linear portion of the profile was utilized to determine the degradation rate  
52  
53 constant (k). Each substrate depletion rate constant was then used to calculate an *in vitro* intrinsic  
54  
55 clearance value ( $CL_{int}$ , *in vitro*) according to the equation,  $CL_{int}$ , *in vitro* = k/microsomal protein  
56  
57  
58  
59  
60

1  
2 content (0.4 mg protein/mL);  $t_{1/2} = \ln(2)/k$ ;  $E_H = CL_{int} / Q + CL_{int}$ .<sup>41</sup> The scaling parameters determined  
3  
4 in literature<sup>42</sup> were used in the aforementioned calculations.  
5  
6  
7

8  
9 **Mouse Model of Malaria Disease Burden.** The method by Fidock *et al.*<sup>27</sup> was followed to  
10 undertake the Peter's 4 day mouse model to evaluate the ability of compounds to suppress malaria  
11 infection. Briefly, male Swiss black mice were infected with *P. berghei* parasites ( $2 \times 10^7$  parasites) by  
12 tail vein injection. For oral administration, an aqueous vehicle containing 0.5% (wt/vol)  
13 hydroxypropyl-methylcellulose (HPMC), 0.4% (vol/vol) Tween 80, and 0.5% (vol/vol) benzyl alcohol  
14 (HPMC-SV) was used. For intraperitoneal administration, a formulation consisting of a 10%  
15 DMSO/90% 5% Solutol HS-15 in 0.9% saline vehicle was used. Compounds **53-56** were administered  
16 at 20 mg/kg. Chloroquine administered at 10 mg/kg was used as a positive control. Formulated drugs  
17 and the vehicle control were then injected either by i.p. or p.o. four hours after infection (day 0) and  
18 then on day 1, 2 and 3. On the fourth day blood smears were taken and parasitemia evaluated.  
19  
20 Microscopic counts of blood films from each mouse were exported into GraphPad Prism (ver 6.05) and  
21 expressed as percentages of parasitemia.  
22  
23  
24  
25  
26  
27  
28  
29  
30  
31  
32  
33  
34  
35  
36  
37  
38  
39

40 **Bioanalysis of blood plasma samples from mouse model.** To determine blood plasma exposure of  
41 compounds, plasma samples were taken from the compound treated parasite infected mice at 2, 5 and  
42 20 h post administration either by i.p. or p.o. Blood samples were collected into EDTA containing  
43 tubes then snap frozen. Samples were thawed and spun down at 13,000 rpm for 10 min and the  
44 supernatant removed and used for analysis. Plasma standards were freshly prepared from a stock  
45 solution (DMSO) for each analytical run with each set of standards comprising at least seven different  
46 analyte concentrations. Plasma standards were then prepared by spiking blank mouse plasma (50  $\mu$ L)  
47 with solution standards (10  $\mu$ L) and the internal standard (IS) diazepam (10  $\mu$ L, 6.25  $\mu$ g/mL in 50%  
48 acetonitrile/water). Plasma samples from the study were similarly prepared except that blank  
49  
50  
51  
52  
53  
54  
55  
56  
57  
58  
59  
60

1  
2 acetonitrile (10  $\mu$ L) was added instead of the solution standard. Protein precipitation for plasma  
3 standards and samples was carried out by the addition of acetonitrile (120  $\mu$ L), vortexing and  
4 centrifugation (10,000 rpm) for 3 minutes in a microcentrifuge. The supernatant was subsequently  
5 separated and 3  $\mu$ L injected directly onto the column for LC-MS analysis. Quantitation of samples was  
6 performed using a Waters Micromass Quattro Premier coupled to a Waters Acquity UPLC coupled to a  
7 positive electrospray ionization multiple-reaction monitoring mode detector. Column used was a  
8 Supelco Ascentis Express RP Amide column (50 x 2.1 mm, 2.7  $\mu$ m); LC conditions used: Gradient  
9 cycle time: 4 min; Injection vol: 3  $\mu$ L; Flow rate: 0.4 mL/min; Mobile phase Acetonitrile-water  
10 gradient with 0.05% formic acid.  
11  
12  
13  
14  
15  
16  
17  
18  
19  
20  
21  
22  
23  
24

25 **General Chemistry Procedures.** Analytical thin-layer chromatography was performed on Merck  
26 silica gel 60F<sup>254</sup> aluminum-backed plates, and visualized by fluorescence quenching under UV light or  
27 by KMnO<sub>4</sub> staining. Flash chromatography was performed with silica gel 60 (particle size 0.040-0.063  
28  $\mu$ m). NMR spectra were recorded on a Bruker Avance DRX 300 with the solvents indicated (<sup>1</sup>H NMR  
29 at 300 MHz). Chemical shifts are reported in ppm on the  $\delta$  scale and referenced to the appropriate  
30 solvent peak. HRMS were acquired by Jason Dang at the Monash Institute of Pharmaceutical Sciences  
31 Spectrometry Facility using an Agilent 1290 infinity 6224 TOF LCMS. Column used was RRHT 2.1 x  
32 50 mm 1.8  $\mu$ m C18. Gradient was applied over the 5 min with the flow rate of 0.5 mL/min. For MS:  
33 Gas temperature was 325°C; drying gas 11 L/min; nebulizer 45 psig and the fragmentor 125V. LCMS  
34 were recorded on a Waters ZQ 3100 using a 2996 Diode Array Detector. LCMS conditions used to  
35 assess purity of compounds were as follows, column: XBridge TM C18 5  $\mu$ m 4.6 x 100 mm, injection  
36 volume 10  $\mu$ L, gradient: 10-100% B over 10 min (solvent A: water 0.1% formic acid; solvent B: AcCN  
37 0.1% formic acid), flow rate: 1.5 mL/min, detection: 100-600 nm. All final compounds were analyzed  
38 using high performance liquid chromatography/ultraviolet/evaporative light scattering detection  
39  
40  
41  
42  
43  
44  
45  
46  
47  
48  
49  
50  
51  
52  
53  
54  
55  
56  
57  
58  
59  
60

1  
2 coupled to mass spectrometry. Unless otherwise noted, all compounds were found to be >95% pure by  
3  
4 this method.  
5  
6

7  
8 The following compounds were purchased commercially and used without further purification, **2-11**,  
9  
10 **14-25** and **28**.

11  
12  
13  
14  
15  
16 **General Procedure A. N4-(Furan-2-ylmethyl)-N2-(4-methoxyphenyl)quinazoline-2,4-diamine (1).**

17  
18 A mixture of N4-(furan-2-ylmethyl)-2-chloroquinazolin-4-amine **57** (50 mg, 0.19 mmol), TFA (60  $\mu$ L,  
19 0.80 mmol) and 4-methoxyaniline (47 mg, 0.39 mmol) in *i*PrOH (3 mL) was stirred under microwave  
20 irradiation (200 W) at 120°C for 15 min. The mixture was partitioned between ethyl acetate (10 mL)  
21 and 10% sodium hydrogen carbonate solution (10 mL). The layers were then separated. The organic  
22 layer was then washed with brine solution (1 x 5 mL). The organic layer was dried (magnesium sulfate)  
23 and the organic layer was concentrated in vacuo to obtain an oil. The oil was subjected to column  
24 chromatography eluting 100% DCM to 10% MeOH/DCM to obtain **1** as a solid (44 mg, 68%). <sup>1</sup>H  
25 NMR (d<sub>6</sub>-DMSO):  $\delta$  8.85 (s, 1H), 8.47 (br s, 1H), 8.05 (d, *J* 8.4 Hz, 1H), 7.75-7.73 (m, 1H), 7.59-7.53  
26 (m, 2H), 7.34 (d, *J* 8.4 Hz, 1H), 7.11 (t, *J* 7.8 Hz, 1H), 6.82 (d, *J* 8.4 Hz, 2H), 6.37-6.32 (m, 2H), 4.73  
27 (d, *J* 6.0 Hz, 2H), 3.68 (s, 3H). MS, *m/z* = 347 [M + H]<sup>+</sup>. HRMS found: (M + H) 347.1506;  
28 C<sub>20</sub>H<sub>18</sub>N<sub>4</sub>O<sub>2</sub> requires (M + H), 347.1508.  
29  
30  
31  
32  
33  
34  
35  
36  
37  
38  
39  
40  
41  
42  
43  
44  
45  
46  
47  
48

49 **N2-(4-Fluorophenyl)-N4-(furan-2-ylmethyl)quinazoline-2,4-diamine (12).** General procedure A  
50 was followed using **57** (100 mg, 0.31 mmol) and 4-fluoroaniline (60  $\mu$ L, 0.63 mmol) to give the title  
51 compound **12** as a white solid (75 mg). <sup>1</sup>H NMR (d<sub>6</sub>-DMSO):  $\delta$  9.11 (s, 1H), 8.56 (t, *J* 5.4 Hz, 1H),  
52 8.12-8.08 (m, 1H), 7.92-7.86 (m, 2H), 7.62-7.57 (m, 2H), 7.42-7.39 (m, 1H), 7.02-7.05 (m, 3H), 6.41-  
53  
54  
55  
56  
57  
58  
59  
60

6.35 (m, 2H), 4.77 (d, *J* 5.7 Hz, 2H). MS,  $m/z = 335 [M + H]^+$ . HRMS found: (M + H) 335.1305;  $C_{19}H_{15}FN_4O$  requires (M + H), 335.1308.

**N4-Benzyl-N2-(4-methoxyphenyl)quinazoline-2,4-diamine (27)**. General procedure A was followed using **58** (100 mg, 0.37 mmol) and 4-methoxyaniline (91 mg, 0.74 mmol) to obtain **27** as a solid (50 mg, 38%).  $^1H$  NMR ( $d_6$ -DMSO):  $\delta$  10.01 (br s, 1H), 8.30 (d, *J* 7.8 Hz, 1H), 7.79-7.76 (m, 1H), 7.55 (d, *J* 7.8 Hz, 1H), 7.45 (d, *J* 7.8 Hz, 2H), 7.43-7.41 (m, 1H), 7.35-7.24 (m, 5H), 7.09 (d, *J* 7.8 Hz, 2H), 6.93-6.91 (m, 1H), 4.75-4.72 (m, 2H), 3.57 (s, 3H). MS,  $m/z = 357 [M + H]^+$ . HRMS found: (M + H) 357.1714;  $C_{22}H_{20}N_4O$  requires (M + H), 357.1715.

**N4-Benzyl-N2-(4-fluorophenyl)quinazoline-2,4-diamine (29)**. General procedure A was followed using **58** (50 mg, 0.19 mmol) and 4-fluoroaniline (18  $\mu$ L, 0.19 mmol) to obtain **29** as a solid (40 mg, 60%).  $^1H$  NMR (MeOD):  $\delta$  7.95 (d, *J* 7.8 Hz, 1H), 7.58-7.56 (m, 1H), 7.51-7.49 (m, 2H), 7.41 (d, *J* 8.4 Hz, 1H), 7.35-7.16 (m, 6H), 6.92-6.89 (m, 2H), 4.80 (m, 2H). MS,  $m/z = 345 [M + H]^+$ . HRMS found: (M + H) 345.1512;  $C_{21}H_{17}N_4F$  requires (M + H), 345.1515.

**N4-Benzyl-N2-[4-(trifluoromethyl)phenyl]quinazoline-2,4-diamine (30)**. General procedure A was followed using **58** (50 mg, 0.19 mmol) and 4-trifluoromethylaniline (60 mg, 0.37 mmol) to obtain **30** as a solid (45 mg, 62%).  $^1H$  NMR ( $d_6$ -DMSO):  $\delta$  10.64 (bs, 1H), 10.40 (bs, 1H), 8.46-8.43 (m, 1H), 7.90-7.50 (m, 7H), 7.38-7.27 (m, 5H), 4.82 (d, *J* 5.9 Hz, 2H). MS,  $m/z = 395 [M + H]^+$ . HRMS found: (M + H) 395.1484;  $C_{22}H_{17}F_3N_4$  requires (M + H), 395.1484.

1  
2 **N4-Benzyl-N2-(4-bromo-3-chlorophenyl)quinazoline-2,4-diamine (31)**. General procedure A was  
3  
4 followed using **58** (60 mg, 0.22 mmol) and 4-bromo-3-chloroaniline (77 mg, 0.44 mmol) to obtain **31**  
5  
6 as a solid (30 mg, 37%). <sup>1</sup>H-NMR (d<sub>6</sub>-DMSO): δ 9.40 (s, 1H), 8.81-8.76 (m, 1H), 8.34 (d, *J* 2.4 Hz,  
7  
8 1H), 8.19-8.16 (m, 1HH), 7.71-7.21 (m, 9H), 4.83 (d, *J* 5.7 Hz, 2H). MS, m/z (%) = 441 (100) [M +  
9  
10 H]<sup>+</sup>, 439 (90), 443 (30), 442 (30). HRMS found: (M + H) 441.0306; C<sub>21</sub>H<sub>16</sub><sup>81</sup>Br<sup>35</sup>ClN<sub>4</sub> requires (M +  
11  
12 H), 441.0305.  
13  
14  
15  
16  
17  
18  
19

20 **N4-Benzyl-N2-(3-chloro-4-fluorophenyl)quinazoline-2,4-diamine (32)**. General procedure A was  
21  
22 followed using **58** (50 mg, 0.19 mmol) and 4-fluoro-3-chloroaniline (54 mg, 0.37 mmol) to obtain **32** as  
23  
24 a solid (65 mg, 93%). <sup>1</sup>H NMR (d<sub>6</sub>-DMSO): δ 10.47 (br s, 1H), 10.38 (br s, 1H), 8.45-8.42 (m, 1H),  
25  
26 7.86-7.83 (m, 2H), 7.63-7.60 (m, 1H), 7.53-7.26 (m, 8H), 4.77 (d, *J* 5.9 Hz, 2H). MS, m/z (%) = 379  
27  
28 (100) [M + H]<sup>+</sup>, 381 (30). HRMS found: (M + H) 379.1123; C<sub>21</sub>H<sub>16</sub><sup>35</sup>ClFN<sub>4</sub> requires (M + H),  
29  
30 379.1126.  
31  
32  
33  
34  
35  
36  
37

38 **N4-Benzyl-N2-(4-chloro-3-fluorophenyl)quinazoline-2,4-diamine (33)**. General procedure A was  
39  
40 followed using **58** (50 mg, 0.19 mmol) and 4-chloro-3-fluoroaniline (54 mg, 0.37 mmol) to obtain **33** as  
41  
42 a solid (65 mg, 93%). <sup>1</sup>H NMR (d<sub>6</sub>-DMSO): δ 9.42 (s, 1H), 8.81-8.76 (m, 1H), 8.19-8.15 (m, 2H),  
43  
44 7.67-7.21 (m, 10H), 4.83 (d, *J* 5.6 Hz, 2H). MS, m/z (%) = 379 (100) [M + H]<sup>+</sup>, 381 (30). HRMS  
45  
46 found: (M + H) 379.1125; C<sub>21</sub>H<sub>16</sub><sup>35</sup>ClFN<sub>4</sub> requires (M + H), 379.1126.  
47  
48  
49  
50  
51  
52  
53

54 **N4-Benzyl-N2-[6-(trifluoromethyl)pyridin-3-yl]quinazoline-2,4-diamine (34)**. General procedure A  
55  
56 was followed using **58** (60 mg, 0.22 mmol) and 6-(trifluoromethyl)pyridin-3-amine (72 mg, 0.44  
57  
58  
59  
60

1  
2 mmol) to obtain **34** as a solid (85 mg, 96%). <sup>1</sup>H NMR (CDCl<sub>3</sub>): δ 8.89 (s, 1H), 8.61-8.58 (m, 1H), 7.69-  
3 7.60 (m, 4H), 7.43-7.28 (m, 5H), 5.99 (br s, 1H), 4.87 (d, *J* 5.4 Hz, 2H). MS, *m/z* = 396 [M + H]<sup>+</sup>.  
4  
5 HRMS found: (M + H) 396.1438; C<sub>21</sub>H<sub>16</sub>F<sub>3</sub>N<sub>5</sub> requires (M + H), 396.1436.  
6  
7  
8  
9

10  
11  
12  
13 **N2-(4-Fluorophenyl)-6,7-dimethoxy-N4-(oxolan-2-ylmethyl)quinazoline-2,4-diamine (35)**. General  
14 procedure A was followed using **59** (100 mg, 0.31 mmol) and 4-fluoroaniline (59 μL, 0.62 mmol) to  
15 obtain **35** as a solid (90 mg, 73%). <sup>1</sup>H NMR (d<sub>6</sub>-DMSO): δ 8.81 (s, 1H), 7.92-7.87 (m, 3H), 7.53 (s,  
16 1H), 7.08-7.01 (m, 2H), 6.81 (s, 1H), 4.17-4.10 (m, 1H), 3.84-3.81 (m, 7H), 3.67-3.53 (m, 3H), 1.95-  
17 1.77 (m, 3H), 1.67-1.58 (m, 1H). MS, *m/z* = 399 [M + H]<sup>+</sup>. HRMS found: (M + H) 399.1834;  
18 C<sub>21</sub>H<sub>23</sub>FN<sub>4</sub>O<sub>3</sub> requires (M + H), 399.1832.  
19  
20  
21  
22  
23  
24  
25  
26  
27  
28  
29  
30

31 **N4-Benzyl-N2-(4-fluorophenyl)-6,7-dimethoxyquinazoline-2,4-diamine (36)**. General procedure A  
32 was followed using **60** (800 mg, 2.43 mmol) and 4-fluoroaniline (461 μL, 4.85 mmol) to obtain **36** as a  
33 solid (850 mg, 87%). <sup>1</sup>H NMR (d<sub>6</sub>-DMSO): δ 8.83 (s, 1H), 8.36-8.32 (m, 1H), 7.87-7.81 (m, 2H), 7.58  
34 (s, 1H), 7.42-7.22 (m, 5H), 7.05-6.99 (m, 2H), 6.85 (s, 1H), 4.80 (d, *J* 5.8 Hz, 2H), 3.88 (s, 3H), 3.84  
35 (s, 3H). MS, *m/z* = 405 [M + H]<sup>+</sup>. HRMS found: (M + H) 405.1727; C<sub>23</sub>H<sub>22</sub>FN<sub>4</sub>O<sub>2</sub> requires (M + H),  
36 405.1727.  
37  
38  
39  
40  
41  
42  
43  
44  
45  
46  
47  
48  
49

50 **N4-Benzyl-N2-(4-fluorophenyl)pyrido[3,4-d]pyrimidine-2,4-diamine (37)**. General procedure A  
51 was followed using **61** (50 mg, 0.19 mmol) and 4-fluoroaniline (41 mg, 0.38 mmol) to obtain **37** as a  
52 solid (40 mg, 63%). <sup>1</sup>H NMR (CDCl<sub>3</sub>): δ 9.02 (s, 1H), 8.35 (d, *J* 5.5 Hz, 1H), 7.71-7.66 (m, 2H), 7.43-  
53  
54  
55  
56  
57  
58  
59  
60

1  
2 7.30 (m, 6H), 7.08-7.01 (m, 3H), 5.93 (br s, 1H), 4.84 (d, *J* 5.5 Hz, 2H). MS, *m/z* = 346 [M + H]<sup>+</sup>.  
3  
4 HRMS found: (M + H) 346.1465; C<sub>20</sub>H<sub>16</sub>FN<sub>5</sub> requires (M + H), 346.1468.  
5  
6  
7  
8  
9

10  
11 **N4-Benzyl-N2-(4-fluorophenyl)pyrido[2,3-d]pyrimidine-2,4-diamine (38)**. General procedure A  
12 was followed using **62** (50 mg, 0.19 mmol) and 4-fluoroaniline (41 mg, 0.38 mmol) to obtain **38** as a  
13 solid (40 mg, 63%). <sup>1</sup>H NMR (CDCl<sub>3</sub>): δ 8.89-8.86 (m, 1H), 7.92 (dd, *J* 8.0 and 1.9 Hz, 1H), 7.75-7.70  
14 (m, 2H), 7.42-7.35 (m, 5H), 7.14-6.99 (m, 4H), 5.95 (br s, 1H), 4.84 (d, *J* 5.4 Hz, 2H). MS, *m/z* = 346  
15 [M + H]<sup>+</sup>. HRMS found: (M + H) 346.1464; C<sub>20</sub>H<sub>16</sub>FN<sub>5</sub> requires (M + H), 346.1468.  
16  
17  
18  
19  
20  
21  
22  
23  
24  
25

26  
27 **N4-Benzyl-N2-(4-fluorophenyl)pyrido[3,2-d]pyrimidine-2,4-diamine (39)**. General procedure A  
28 was followed using **63** (50 mg, 0.19 mmol) and 4-fluoroaniline (41 mg, 0.38 mmol) to obtain **39** as a  
29 solid (40 mg, 63%). <sup>1</sup>H NMR (CDCl<sub>3</sub>): δ 8.39-8.37 (m, 1H), 7.80 (dd, *J* 8.5 and 1.5 Hz, 1H), 7.67-62  
30 (m, 2H), 7.51-7.30 (m, 7H), 7.08-6.97 (m, 3H), 4.80 (d, *J* 5.9 Hz, 2H). MS, *m/z* = 346 [M + H]<sup>+</sup>.  
31  
32 HRMS found: (M + H) 346.1466; C<sub>20</sub>H<sub>16</sub>FN<sub>5</sub> requires (M + H), 346.1468.  
33  
34  
35  
36  
37  
38  
39  
40  
41

42  
43 **N4-Benzyl-N2-(4-fluorophenyl)thieno[3,2-d]pyrimidine-2,4-diamine (40)**. General procedure A was  
44 followed using **64** (50 mg, 0.18 mmol) and 4-fluoroaniline (40 mg, 0.36 mmol) to obtain **40** as a solid  
45 (35 mg, 55%). <sup>1</sup>H NMR (CDCl<sub>3</sub>): δ 7.64 (d, *J* 5.3 Hz, 1H), 7.59-7.54 (m, 2H), 7.40-7.30 (m, 5H), 7.22  
46 (d, *J* 5.3 Hz, 1H), 7.02-6.96 (m, 3H), 5.65 (br s, 1H), 4.84 (d, *J* 5.6 Hz, 2H). MS, *m/z* = 351 [M + H]<sup>+</sup>.  
47  
48 HRMS found: (M + H) 351.1081; C<sub>19</sub>H<sub>15</sub>FN<sub>4</sub>S requires (M + H), 351.1080.  
49  
50  
51  
52  
53  
54  
55  
56  
57  
58  
59  
60

**N6-Benzyl-N2-(4-fluorophenyl)-7-methyl-7H-purine-2,6-diamine (41).** General procedure A was followed using **65** (50 mg, 0.18 mmol) and 4-fluoroaniline (41 mg, 0.36 mmol) to obtain **41** as an oil (40 mg, 63%). <sup>1</sup>H NMR (CDCl<sub>3</sub>): δ 7.77 (s, 1H), 7.62-7.56 (m, 1H), 7.39-7.33 (m, 5H), 7.10-7.04 (m, 1H), 6.95-6.85 (m, 2H), 4.83-4.79 (m, 2H), 4.02-3.96 (m, 3H). MS, m/z = 349 [M + H]<sup>+</sup>. HRMS found: (M + H) 349.1578; C<sub>19</sub>H<sub>17</sub>FN<sub>6</sub> requires (M + H), 349.1577.

**N4-Benzyl-N6-(4-fluorophenyl)-1-methyl-1H-pyrazolo[3,4-d]pyrimidine-4,6-diamine (42).**

General procedure A was followed using **66** (50 mg, 0.18 mmol) and 4-fluoroaniline (41 mg, 0.36 mmol) to obtain **42** as an oil (45 mg, 71%). <sup>1</sup>H NMR (CDCl<sub>3</sub>): δ 7.68 (s, 1H), 7.62-7.57 (m, 2H), 5.37-7.25 (m, 5H), 7.07 (br s, 1H), 7.01-6.95 (m, 2H), 5.65 (br s, 1H), 4.77 (d, J 5.7 Hz, 2H), 3.90 (s, 3H). MS, m/z = 349 [M + H]<sup>+</sup>. HRMS found: (M + H) 349.1577; C<sub>19</sub>H<sub>17</sub>FN<sub>6</sub> requires (M + H), 349.1577.

**N2-(3-Chloro-4-fluorophenyl)-N4-(2-(4-methylpiperazin-1-yl)ethyl)pyrido[3,2-d]pyrimidine-2,4-diamine (43).** General procedure A was followed using **67** (50 mg, 0.16 mmol) and 3-chloro-4-fluoroaniline (47 mg, 0.32 mmol) to obtain **43** as a solid (45 mg, 66%). <sup>1</sup>H NMR (CDCl<sub>3</sub>): δ 8.44 (d, J 4.2 and 1.5 Hz, 1H), 8.08 (d, J 6.7 and 2.7 Hz, 1H), 7.83-7.79 (m, 2H), 7.53-7.48 (m, 1H), 7.44-7.38 (m, 1H), 7.30 (br s, 1H), 7.07 (t, J 8.8 Hz, 1H), 3.70 (q, J 6.3 Hz, 2H), 2.73 (t, J 6.3 Hz, 2H), 2.60-2.50 (m, 8H), 2.33 (s, 1H). MS, m/z (%) = 416 [M + H]<sup>+</sup> (100), 418 (30). HRMS found: (M + H) 416.1766; C<sub>20</sub>H<sub>23</sub><sup>35</sup>ClFN<sub>7</sub> requires (M + H), 416.1766.

**N2-(4-Chloro-3-fluorophenyl)-N4-(2-(4-methylpiperazin-1-yl)ethyl)pyrido[3,2-d]pyrimidine-2,4-diamine (44).** General procedure A was followed using **68** (50 mg, 0.16 mmol) and 4-chloro-3-fluoro-

1  
2 aniline (47 mg, 0.32 mmol) to obtain **44** as a solid (30 mg, 44%). <sup>1</sup>H NMR (CDCl<sub>3</sub>): δ 8.47 (dd, *J* 4.3  
3 and 1.5 Hz, 1H), 8.13-8.08 (m, 1H), 7.86-7.83 (m, 1H), 7.55-7.51 (m, 2H), 7.31-7.15 (m, 2H), 3.71 (q,  
4 *J* 6.3 Hz, 2H), 2.75 (t, *J* 6.3 Hz, 2H), 2.65-2.55 (m, 8H), 2.35 (s, 3H). MS, *m/z* (%) = 416 [M + H]<sup>+</sup>  
5 (100), 418 (30). HRMS found: (M + H) 416.1765; C<sub>20</sub>H<sub>23</sub><sup>35</sup>ClFN<sub>7</sub> requires (M + H), 416.1766.  
6  
7  
8  
9  
10  
11  
12  
13  
14

#### 15 **N2-(3-Chloro-4-fluorophenyl)-N4-(1-methylpiperidin-4-yl)pyrido[3,2-d]pyrimidine-2,4-diamine**

16 **(45)**. General procedure A was followed using **69** (50 mg, 0.18 mmol) and 3-chloro-4-fluoro-aniline  
17 (52 mg, 0.36 mmol) to obtain **45** as a solid (35 mg, 50%). <sup>1</sup>H NMR (CDCl<sub>3</sub>): δ 8.43 (dd, *J* 4.3 and 1.5  
18 Hz, 1H), 8.15 (dd, *J* 6.7 and 2.7 Hz, 1H), 7.80 (dd, *J* 8.4 and 1.5 Hz), 7.53-7.49 (m, 1H), 7.35-2.29 (m,  
19 2H), 7.10-7.04 (m, 2H), 4.15-4.06 (m, 1H), 2.95-2.90 (m, 2H), 2.37 (s, 3H), 2.31-2.15 (m, 4H), 1.85-  
20 1.72 (m, 2H). MS, *m/z* (%) = 385 (100) [M + H]<sup>+</sup>, 387 (30). HRMS found: (M + H) 387.1500;  
21 C<sub>19</sub>H<sub>20</sub><sup>35</sup>ClFN<sub>6</sub> requires (M + H), 387.1500.  
22  
23  
24  
25  
26  
27  
28  
29  
30  
31  
32  
33  
34  
35

#### 36 **N2-(3-Fluoro-4-chlorophenyl)-N4-(1-methylpiperidin-4-yl)pyrido[3,2-d]pyrimidine-2,4-diamine**

37 **(46)**. General procedure A was followed using **68** (50 mg, 0.18 mmol) and 4-chloro-3-fluoro-aniline  
38 (52 mg, 0.36 mmol) to obtain **46** as a solid (25 mg, 36%). <sup>1</sup>H NMR (CDCl<sub>3</sub>): δ 8.45 (dd, *J* 4.3 and 1.5  
39 Hz, 1H), 8.14 (dd, *J* 12.1 and 2.4 Hz, 1H), 7.84 (dd, *J* 8.5 and 1.5 Hz, 1H), 7.55-7.51 (m, 1H), 7.30 (br  
40 s, 1H), 7.30-7.25 (m, 1H), 7.15-7.05 (m, 2H), 4.14-4.07 (m, 1H), 2.97-2.93 (m, 2H), 2.39 (s, 3H), 2.31-  
41 2.16 (m, 4H), 1.88-1.75 (m, 2H). MS, *m/z* (%) = 385 (100) [M + H]<sup>+</sup>, 387 (30). HRMS found: (M + H)  
42 387.1499; C<sub>19</sub>H<sub>20</sub><sup>35</sup>ClFN<sub>6</sub> requires (M + H), 387.1500.  
43  
44  
45  
46  
47  
48  
49  
50  
51  
52  
53  
54  
55  
56  
57  
58  
59  
60

1  
2 **N4-[2-(Dimethylamino)ethyl]-N2-(4-fluorophenyl)quinazoline-2,4-diamine (47)**. General procedure  
3  
4 A was followed using **69** (50 mg, 0.20 mmol) and 4-fluoroaniline (44 mg, 0.40 mmol) to obtain **47** as  
5  
6 an oil (46 mg, 71%). <sup>1</sup>H NMR (CDCl<sub>3</sub>): δ 7.85 (br s, 1H), 7.72-7.57 (m, 5H), 7.22-7.16 (m, 1H), 7.06-  
7  
8 6.99 (m, 2H), 6.76 (br s, 1H), 3.68-2.62 (m, 2H), 2.65 (t, *J* 6.1 Hz, 2H), 2.33 (s, 6H). MS, *m/z* = 326  
9  
10 [M + H]<sup>+</sup>. HRMS found: (M + H) 326.1779; C<sub>18</sub>H<sub>20</sub>FN<sub>5</sub> requires (M + H), 326.1781.  
11  
12  
13  
14  
15  
16  
17

18 **N2-(4-Fluorophenyl)-N4-[2-(4-methylpiperazin-1-yl)ethyl]quinazoline-2,4-diamine (48)**. General  
19  
20 procedure A was followed using **70** (50 mg, 0.16 mmol) and 4-fluoroaniline (36 mg, 0.33 mmol) to  
21  
22 obtain **48** as an oil (20 mg, 32%). <sup>1</sup>H NMR (CDCl<sub>3</sub>): δ 7.74-7.55 (m, 5H), 7.25-7.19 (m, 1H), 7.10 (br  
23  
24 s, 1H), 7.07-7.03 (m, 2H), 6.57 (br s, 1H), 3.70-3.64 (m, 2H), 2.74 (t, *J* 6.1 Hz, 2H), 2.64-2.50 (m, 8H),  
25  
26 2.35 (s, 3H). MS, *m/z* = 381 [M + H]<sup>+</sup>. HRMS found: (M + H) 381.2202; C<sub>21</sub>H<sub>25</sub>FN<sub>6</sub> requires (M + H),  
27  
28 381.2203.  
29  
30  
31  
32  
33  
34  
35

36 **N2-(4-Fluorophenyl)-N4-[2-(morpholin-4-yl)ethyl]quinazoline-2,4-diamine (49)**. General  
37  
38 procedure A was followed using **71** (50 mg, 0.17 mmol) and 4-fluoroaniline (38 mg, 0.34 mmol) to  
39  
40 obtain **49** as a solid (60 mg, 95%). <sup>1</sup>H NMR (CDCl<sub>3</sub>): δ 7.73-7.57 (m, 5H), 7.30 (br s 1H), 7.25-7.19  
41  
42 (m, 1H), 7.06-7.00 (m, 2H), 6.53 (br s, 1H), 3.81-3.77 (m, 4H), 3.72-3.66 (m, 2H), 2.76-2.71 (m, 2H),  
43  
44 2.58-2.55 (m, 4H). MS, *m/z* = 368 [M + H]<sup>+</sup>. HRMS found: (M + H) 368.1885; C<sub>20</sub>H<sub>22</sub>FN<sub>5</sub>O requires  
45  
46 (M + H), 368.1887.  
47  
48  
49  
50  
51  
52  
53

54 **N2-(4-Fluorophenyl)-N4-(2-(pyrrolidin-1-yl)ethyl)quinazoline-2,4-diamine (50)**. General procedure  
55  
56 A was followed using **72** (50 mg, 0.18 mmol) and 4-fluoroaniline (40 mg, 0.36 mmol) to obtain **50** as  
57  
58  
59  
60

1  
2 an oil (50 mg, 79%).  $^1\text{H}$  NMR ( $\text{CDCl}_3$ ):  $\delta$  7.73-7.54 (m, 5H), 7.23-7.17 (m, 1H), 7.05-7.00 (m, 2H),  
3  
4 6.86 (br s, 1H), 3.74-3.70 (m, 2H), 4.30 (br s, 1H), 2.90-2.86 (m, 2H), 2.70-2.65 (m, 4H), 1.89-1.85 (m,  
5  
6 4H). MS,  $m/z = 352$   $[\text{M} + \text{H}]^+$ . HRMS found: (M + H) 352.1935;  $\text{C}_{20}\text{H}_{22}\text{FN}_5$  requires (M + H),  
7  
8 352.1937.  
9

10  
11  
12  
13  
14  
15  
16 **2-((2-[(4-Fluorophenyl)amino]quinazolin-4-yl)amino)-1-(4-methylpiperazin-1-yl)ethan-1-one**

17  
18 **(51)**. General procedure A was followed using **73** (50 mg, 0.16 mmol) and 4-fluoroaniline (35 mg, 0.32  
19  
20 mmol) to obtain **51** as a solid (20 mg, 32%).  $^1\text{H}$  NMR ( $\text{CDCl}_3$ ):  $\delta$  7.76-7.58 (m, 5H), 7.27-7.01 (m,  
21  
22 5H), 4.34-4.32 (m, 2H), 3.78-3.74 (m, 2H), 3.55-3.52 (m, 2H), 2.49-2.45 (m, 4H), 2.37 (s, 3H). MS,  
23  
24  $m/z = 395$   $[\text{M} + \text{H}]^+$ . HRMS found: (M + H) 395.1993;  $\text{C}_{21}\text{H}_{23}\text{FN}_6\text{O}$  requires (M + H), 395.1996.  
25  
26  
27  
28  
29  
30

31  
32 **N2-(4-Fluorophenyl)-N4-(1-methylpiperidin-4-yl)quinazoline-2,4-diamine (52)**. General procedure  
33  
34 A was followed using **74** (50 mg, 0.18 mmol) and 4-fluoroaniline (40 mg, 0.36 mmol) to obtain **52** as a  
35  
36 solid (40 mg, 63%).  $^1\text{H}$  NMR ( $\text{CDCl}_3$ ):  $\delta$  7.71-7.54 (m, 5H), 7.21-7.15 (m, 2H), 7.05 (m, 2H), 5.57-  
37  
38 5.52 (m, 1H), 4.21-4.15 (m, 1H), 2.93-2.88 (m, 2H), 2.35 (s, 3H), 2.23-2.16 (m, 4H), 1.74-1.62 (m,  
39  
40 2H). MS,  $m/z = 352$   $[\text{M} + \text{H}]^+$ . HRMS found: (M + H) 352.1935;  $\text{C}_{20}\text{H}_{22}\text{FN}_5$  requires (M + H),  
41  
42 352.1937.  
43  
44  
45  
46  
47  
48  
49

50  
51 **N2-(3-Chloro-4-fluorophenyl)-N4-[2-(4-methylpiperazin-1-yl)ethyl]quinazoline-2,4-diamine bis**  
52  
53 **hydrochloride (53)**. General procedure A was followed using **70** (120 mg, 0.39 mmol) and 3-chloro-4-  
54  
55 fluoro-aniline (114 mg, 0.78 mmol) to obtain the free base of **53** as an oil (75 mg, 46%).  $^1\text{H}$  NMR  
56  
57 ( $\text{CDCl}_3$ ):  $\delta$  8.07 (dd,  $J$  6.7 and 2.7 Hz, 1H), 7.62-7.52 (m, 3H), 7.40-7.35 (m, 1H), 7.26-7.17 (m, 1H),  
58  
59  
60

1  
2 7.02 (t, *J* 8.8 Hz, 1H), 6.65 (br s, 1H), 3.68-3.62 (m, 2H), 2.71 (t, *J* 6.1 Hz, 2H), 2.58-2.48 (m, 8H),  
3  
4 2.31 (s, 3H). MS, *m/z* (%) = 415 (100) [M + H]<sup>+</sup>, 417 (30). For animal studies the compound was  
5  
6 converted to the bis hydrochloride salt **53**. HRMS found: (M + H) 415.1813; C<sub>21</sub>H<sub>24</sub><sup>35</sup>ClFN<sub>6</sub> requires  
7  
8 (M + H), 415.1813.  
9  
10

11  
12  
13  
14  
15 **N2-(4-Chloro-3-fluorophenyl)-N4-[2-(4-methylpiperazin-1-yl)ethyl]quinazoline-2,4-diamine bis**  
16  
17 **hydrochloride (54)**. General procedure A was followed using **70** (120 mg, 0.39 mmol) and 4-chloro-3-  
18  
19 fluoro-aniline (114 mg, 0.78 mmol) to obtain the free base of **54** as a solid (45 mg, 28%). <sup>1</sup>H NMR  
20  
21 (CDCl<sub>3</sub>): δ 8.08 (dd, *J* 12.2 and 2.4 Hz, 1H), 7.61-7.56 (m, 3H), 7.26-7.12 (m, 4H), 6.65 (br s, 1H),  
22  
23 3.69-3.63 (m, 2H), 2.73 (t, *J* 6.2 Hz, 2H), 2.59-2.51 (m, 8H), 2.33 (s, 3H). MS, *m/z* (%) = 415 (100) [M  
24  
25 + H]<sup>+</sup>, 417 (30). For animal studies the compound was converted to the bis hydrochloride salt **54**.  
26  
27 HRMS found: (M + H) 415.1812; C<sub>21</sub>H<sub>24</sub><sup>35</sup>ClFN<sub>6</sub> requires (M + H), 415.1813.  
28  
29  
30  
31  
32  
33  
34  
35

36 **N2-(3-Chloro-4-fluorophenyl)-N4-(1-methylpiperidin-4-yl)quinazoline-2,4-diamine**  
37  
38 **hydrochloride (55)**. General procedure A was followed using **74** (90 mg, 0.33 mmol), and 3-chloro-4-  
39  
40 fluoro-aniline (95 mg, 0.65 mmol) to obtain the free base of **55** as a solid (25 mg, 20%). <sup>1</sup>H NMR  
41  
42 (CDCl<sub>3</sub>): δ 8.12 (dd, *J* 6.7 and 2.7 Hz, 1H), 7.63-7.45 (m, 3H), 7.34-7.29 (m, 1H), 7.23-7.17 (m, 1H),  
43  
44 7.10-7.03 (m, 2H), 5.55 (br s, 1H), 4.22-4.15 (m, 1H), 2.93-2.89 (m, 2H), 2.34 (s, 3H), 2.34-2.15 (m,  
45  
46 4H), 1.75-1.63 (m, 2H). MS, *m/z* (%) = 384 (100) [M + H]<sup>+</sup>, 386 (30). For animal studies the  
47  
48 compound was converted to the bis hydrochloride salt **55**. HRMS found: (M + H) 386.1545;  
49  
50 C<sub>20</sub>H<sub>21</sub><sup>35</sup>ClFN<sub>5</sub> requires (M + H), 386.1548.  
51  
52  
53  
54  
55  
56  
57  
58  
59  
60

**N2-(4-Chloro-3-fluorophenyl)-N4-(1-methylpiperidin-4-yl)quinazoline-2,4-diamine**

**hydrochloride (56).** General procedure A was followed using **74** (90 mg, 0.33 mmol) and 4-chloro-3-fluoro-aniline (95 mg, 0.65 mmol) to obtain the free base of **56** as a solid (45 mg, 36%). <sup>1</sup>H NMR (CDCl<sub>3</sub>): δ 8.11 (dd, *J* 12.2 and 2.5 Hz, 1H), 7.63-7.54 (m, 4H), 7.26-7.18 (m, 2H), 7.10-7.06 (m, 1H), 5.66-5.63 (br s, 1H), 4.23-4.13 (m, 1H), 2.96-2.91 (m, 2H), 2.36 (s, 3H), 2.29-2.16 (m, 4H), 1.78-1.65 (m, 2H). MS, *m/z* (%) = 384 (100) [M + H]<sup>+</sup>, 386 (30). For animal studies the compound was converted to the bis hydrochloride salt **56**. HRMS found: (M + H) 386.1545; C<sub>20</sub>H<sub>21</sub><sup>35</sup>ClFN<sub>5</sub> requires (M + H), 386.1548.

**General Procedure B. N4-(Furan-2-ylmethyl)-2-chloroquinazolin-4-amine (57).** A mixture of 2,4-dichloroquinazoline (2.0 g, 10.0 mmol), furfurylamine (1.33 mL, 15.1 mmol), and DIPEA (2.6 mL, 15.1 mmol) in acetonitrile (20 mL) was allowed to stir for 18 h at 20 °C. 10% citric acid solution (10 mL) was added and the solution extracted with EtOAc (2 x 10 mL). The organic layer was dried with MgSO<sub>4</sub> and concentrated *in vacuo*. The resulting residue was purified using column chromatography gradient eluting from 100% DCM to 5% MeOH/DCM to obtain **57** as a solid (2.45 g). <sup>1</sup>H NMR (d<sub>6</sub>-DMSO): δ 9.19 (br s, 1H), 8.27 (d, *J* 8.4 Hz, 1H), 7.80-7.46 (m, 4H), 6.40-6.34 (m, 2H), 4.71 (d, *J* 5.4 Hz, 2H). MS, *m/z* (%) = 260 (100) [M + H]<sup>+</sup>, 32 (30).

**N-Benzyl-2-chloroquinazolin-4-amine (58).** General procedure B was followed using 2,4-dichloroquinazoline (500 mg, 2.51 mmol) and benzylamine (274 μL, 2.51 mmol) to obtain **58** as a solid (426 mg, 63%). <sup>1</sup>H NMR (d<sub>6</sub>-DMSO): δ 9.27 (brs, 1H), 8.30-8.28 (m, 1H), 7.79-7.71 (m, 1H), 7.62-7.61 (m, 1H), 7.54-7.51 (m, 1H), 7.36-7.30 (m, 4H), 7.25-7.22 (m, 1H), 4.74 (s, 2H). MS, *m/z* (%) = 270 (100) [M + H]<sup>+</sup>, 272 (30).

1  
2  
3  
4  
5 **2-Chloro-6,7-dimethoxy-N-((tetrahydrofuran-2-yl)methyl)quinazolin-4-amine (59)**. General  
6  
7 procedure B was followed using 2,4-dichloro-6,7-dimethoxyquinazoline (500 mg, 1.93 mmol) and  
8  
9 tetrahydrofurfurylamine (351 mg, 3.47 mmol) to obtain **59** as a foam (610 mg, 97%). <sup>1</sup>H NMR (d<sub>6</sub>-  
10  
11 DMSO): δ 8.47-8.44 (m, 1H), 7.67 (s, 1H), 7.05 (s, 1H), 4.11-4.05 (m, 1H), 3.84 (s, 6H), 3.84-3.76 (m,  
12  
13 1H), 3.67-3.50 (m, 3H), 1.93-1.77 (m, 3H), 1.65-1.56 (m, 1H). MS, m/z (%) = 324 (100) [M + H]<sup>+</sup>,  
14  
15 326 (30).  
16  
17  
18  
19  
20  
21  
22

23 **N-Benzyl-2-chloro-6,7-dimethoxyquinazolin-4-amine (60)**. General procedure B was followed using  
24  
25 2,4-dichloro-6,7-dimethoxyquinazoline (2.0 g, 7.72 mmol) and benzylamine (1.52 mL, 13.89 mmol) to  
26  
27 obtain **60** as a solid (2.45 g, 96%). <sup>1</sup>H NMR (d<sub>6</sub>-DMSO): δ 8.90-8.85 (m, 1H), 7.69 (s, 1H), 7.41-7.24  
28  
29 (m, 5H), 7.10 (s, 1H), 4.75 (d, *J* 5.8 Hz, 2H), 3.90 (s, 3H), 3.88 (s, 3H). MS, m/z (%) = 330 (100) [M +  
30  
31 H]<sup>+</sup>, 332 (40).  
32  
33  
34  
35  
36  
37  
38

39 **N-Benzyl-2-chloropyrido[3,4-d]pyrimidin-4-amine (61)**. General procedure B was followed using  
40  
41 2,4-dichloropyrido[3,4-d]pyrimidine (100 mg, 0.50 mmol) and benzylamine (60 μL, 0.55 mmol) to  
42  
43 obtain **61** as a foam (80 mg, 59%). <sup>1</sup>H NMR (CDCl<sub>3</sub>): δ 9.22 (s, 1H), 8.62 (d, *J* 5.6 Hz, 1H), 7.47-7.39  
44  
45 (m, 6H), 6.22 (brs, 1H), 4.89 (d, *J* 5.3 Hz, 2H). MS, m/z (%) = 271 (100) [M + H]<sup>+</sup>, 273 (30).  
46  
47  
48  
49  
50  
51  
52

53 **N-Benzyl-2-chloropyrido[2,3-d]pyrimidin-4-amine (62)**. General procedure B was followed using  
54  
55 2,4-dichloropyrido[2,3-d]pyrimidine (100 mg, 0.5 mmol) and benzylamine (60 μL, 0.55 mmol) to  
56  
57 obtain **62** as a solid (120 mg, 89%). <sup>1</sup>H NMR (d<sub>6</sub>-DMSO): δ 9.58-9.54 (m, 1H), 9.98 (dd, *J* 6.3 and 1.9  
58  
59  
60

1  
2 Hz, 1H), 8.77 (dd, *J* 8.3 and 1.9 Hz, 1H), 7.58 (dd, *J* 8.42 and 4.4 Hz, 1H), 7.41-7.27 (m, 5H), 4.77 (d,  
3  
4 *J* 5.8 Hz, 2H). MS, *m/z* (%) = 271 (100) [M + H]<sup>+</sup>, 273 (30).  
5  
6  
7  
8  
9

10  
11 **N-Benzyl-2-chloropyrido[3,2-d]pyrimidin-4-amine (63)**. General procedure B was followed using  
12  
13 2,4-dichloropyrido[3,2-d]pyrimidine (100 mg, 0.5 mmol) and benzylamine (60 μL, 0.55 mmol) to  
14  
15 obtain **63** as a solid (100 mg, 74%). <sup>1</sup>H NMR (CDCl<sub>3</sub>): δ 8.66-8.64 (m, 1H), 8.06-8.02 (m, 1H), 7.68-  
16  
17 7.63 (m, 2H), 7.45-7.32 (m, 5H), 4.86 (d, *J* 5.9 Hz, 2H). MS, *m/z* (%) = 271 (100) [M + H]<sup>+</sup>, 273 (30).  
18  
19  
20  
21  
22  
23

24  
25 **N-Benzyl-2-chlorothieno[3,2-d]pyrimidin-4-amine (64)**. General procedure B was followed using  
26  
27 2,4-dichlorothieno[3,2-d]pyrimidine (100 mg, 0.49 mmol) and benzylamine (60 μL, 0.55 mmol) to  
28  
29 obtain **64** as a solid (90 mg, 67%). <sup>1</sup>H NMR (CDCl<sub>3</sub>): δ 7.76 (d, *J* 5.4 Hz, 1H), 7.44-7.38 (m, 6H), 5.40  
30  
31 (brs, 1H), 4.89 (d, *J* 5.6 Hz, 2H). MS, *m/z* (%) = 276 (100) [M + H]<sup>+</sup>, 278 (60).  
32  
33  
34  
35  
36  
37

38  
39 **N-Benzyl-2-chloro-7-methyl-7H-purin-6-amine (65)**. General procedure B was followed using 2,6-  
40  
41 dichloro-7-methyl-7H-purine (100 mg, 0.49 mmol) and benzylamine (60 μL, 0.55 mmol) to obtain **65**  
42  
43 as a solid (120 mg, 89%). <sup>1</sup>H NMR (CDCl<sub>3</sub>): δ 7.81 (s, 1H), 7.44-7.37 (m, 5H), 5.33-5.31 (brs, 1H),  
44  
45 4.87-4.84 (m, 2H), 4.04 (s, 3H). MS, *m/z* (%) = 274 (100) [M + H]<sup>+</sup>, 276 (40).  
46  
47  
48  
49  
50  
51

52  
53 **N-Benzyl-6-chloro-1-methyl-1H-pyrazolo[3,4-d]pyrimidin-4-amine (66)**. General procedure B was  
54  
55 followed using 4,6-dichloro-1-methyl-1H-pyrazolo[3,4-d]pyrimidine (100 mg, 0.49 mmol) and  
56  
57 benzylamine (60 μL, 0.55 mmol) to obtain **66** as an oil (120 mg, 89%). <sup>1</sup>H NMR (CDCl<sub>3</sub>): δ 7.80 (s,  
58  
59  
60

1  
2 1H), 7.39-7.30 (m, 5H), 5.95 (brs, 1H), 4.86 (d, *J* 5.8 Hz, 2H), 3.98 (s, 3H). MS, *m/z* (%) = 274 (100)  
3  
4 [M + H]<sup>+</sup>, 276 (60).  
5  
6  
7  
8  
9

10 **2-Chloro-N-(2-(4-methylpiperazin-1-yl)ethyl)pyrido[3,2-d]pyrimidin-4-amine (67)**. General  
11 procedure B was followed using 2,4-dichloropyrido[3,2-d]pyrimidine (200 mg, 1.00 mmol) and 2-(4-  
12 methylpiperazin-1-yl)ethanamine (186 μL, 1.30 mmol) to obtain **67** as a solid (170 mg, 56%). <sup>1</sup>H NMR  
13 (CDCl<sub>3</sub>): δ 8.71 (dd, *J* 4.3 and 1.5 Hz, 1H), 8.02 (dd, *J* 8.5 and 1.6 Hz, 1H), 7.82 (brs, 1H), 7.66 (dd, *J*  
14 8.5 and 4.3 Hz, 1H), 3.78-3.73 (m, 2H), 2.74 (t, *J* 6.2 Hz, 3H), 2.70-2.50 (m, 8H), 2.37 (s, 3H). MS,  
15 *m/z* (%) = 307 (100) [M + H]<sup>+</sup>, 309 (30).  
16  
17  
18  
19  
20  
21  
22  
23  
24  
25  
26  
27  
28

29 **2-Chloro-N-(1-methylpiperidin-4-yl)pyrido[3,2-d]pyrimidin-4-amine (68)**. General procedure B  
30 was followed using 2,4-dichloropyrido[3,2-d]pyrimidine (200 mg, 1.0 mmol) and 1-methylpiperidin-4-  
31 amine (148 mg, 1.30 mmol) to obtain **68** as a solid (230 mg, 83%). <sup>1</sup>H NMR (CDCl<sub>3</sub>): δ 8.70 (dd, *J* 4.3  
32 and 1.6 Hz, 1H), 8.03 (dd, *J* 6.4 and 1.6 Hz, 1H), 7.67 (dd, *J* 8.5 and 4.3 Hz, 1H), 7.25 (brs, 1H), 4.32-  
33 4.22 (m, 1H), 2.99-2.94 (m, 2H), 2.41 (s, 3H), 2.40-2.16 (m, 4H), 1.89-1.77 (m, 2H). MS, *m/z* (%) =  
34 278 (100) [M + H]<sup>+</sup>, 280 (30).  
35  
36  
37  
38  
39  
40  
41  
42  
43  
44  
45  
46

47 **N1-(2-Chloroquinazolin-4-yl)-N2,N2-dimethylethane-1,2-diamine (69)**. General procedure B was  
48 followed using 2,4-dichloroquinazoline (150 mg, 0.75 mmol) and N,N-dimethylethylenediamine (79  
49 μL, 0.98 mmol) to obtain **69** as a solid (155 mg, 82%). <sup>1</sup>H NMR (CDCl<sub>3</sub>): δ 7.80-7.70 (m, 3H), 7.50-  
50 7.44 (m, 1H), 6.96 (brs, 1H), 3.73-3.68 (m, 2H), 2.68-2.64 (m, 2H), 2.35 (s, 6H). MS, *m/z* (%) = 251  
51 (100) [M + H]<sup>+</sup>, 253 (30).  
52  
53  
54  
55  
56  
57  
58  
59  
60

1  
2  
3  
4  
5 **2-Chloro-N-(2-(4-methylpiperazin-1-yl)ethyl)quinazolin-4-amine (70)**. General procedure B was  
6 followed using 2,4-dichloroquinazoline (150 mg, 0.75 mmol) and 2-(4-methylpiperazin-1-  
7 yl)ethanamine (140 mg, 0.98 mmol) to obtain **70** as an oil (150 mg, 65%). <sup>1</sup>H NMR (CDCl<sub>3</sub>): δ 7.80-  
8 7.71 (m, 3H), 7.53-7.48 (m, 1H), 6.99 (brs, 1H), 3.76-3.70 (m, 2H), 2.78-2.73 (m, 2H), 2.70-2.50 (m,  
9 8H), 2.36 (s, 3H). MS, m/z = 306 [M + H]<sup>+</sup>.  
10  
11  
12  
13  
14  
15  
16  
17  
18  
19  
20

21 **2-Chloro-N-(2-morpholinoethyl)quinazolin-4-amine (71)**. General procedure B was followed using  
22 2,4-dichloroquinazoline (150 mg, 0.75 mmol) and 4-(2-aminoethyl)morpholine (128 mg, 0.98 mmol) to  
23 obtain **71** as a solid (170 mg, 77%). <sup>1</sup>H NMR (CDCl<sub>3</sub>): δ 7.82-7.72 (m, 3H), 7.68-7.48 (m, 1H), 6.86  
24 (brs, 1H), 3.82-3.73 (m, 6H), 2.77-2.73 (m, 2H), 2.61-2.57 (m, 4H). MS, m/z (%) = 293 (100) [M +  
25 H]<sup>+</sup>, 295 (30).  
26  
27  
28  
29  
30  
31  
32  
33  
34  
35  
36

37 **2-Chloro-N-(2-(pyrrolidin-1-yl)ethyl)quinazolin-4-amine (72)**. General procedure B was followed  
38 using 2,4-dichloroquinazoline (150 mg, 0.75 mmol) and 2-(pyrrolidin-1-yl)ethanamine (112 mg, 0.98  
39 mmol) to obtain **72** as a solid (135 mg, 65%). <sup>1</sup>H NMR (CDCl<sub>3</sub>): δ 7.74-7.66 (m, 3H), 7.45-7.39 (m,  
40 1H), 7.05 (brs, 1H), 3.74-3.69 (m, 2H), 2.85-2.81 (m, 2H), 2.65-2.60 (m, 4H), 1.85-1.80 (m, 4H). MS,  
41 m/z (%) = 279 (100) [M + H]<sup>+</sup>, 281 (30).  
42  
43  
44  
45  
46  
47  
48  
49  
50  
51  
52

53 **2-(2-Chloroquinazolin-4-ylamino)-1-(4-methylpiperazin-1-yl)ethanone (73)**. General procedure B  
54 was followed using 2,4-dichloroquinazoline (150 mg, 0.75 mmol) and 2-amino-1-(4-methylpiperazin-  
55 1-yl)ethanone bis hydrochloride (225 mg, 0.98 mmol) to obtain **73** as a solid (135 mg, 56%). <sup>1</sup>H NMR  
56  
57  
58  
59  
60

(CDCl<sub>3</sub>): δ 7.88-7.84 (m, 1H), 7.77-7.75 (m, 2H), 7.51-7.47 (m, 2H), 4.39-4.38 (m, 2H), 3.78-3.75 (m, 2H), 3.61-3.58 (m, 2H), 2.52-2.48 (m, 4H), 2.37 (s, 3H). MS, m/z (%) = 320 (100) [M + H]<sup>+</sup>, 322 (30).

**2-Chloro-N-(1-methylpiperidin-4-yl)quinazolin-4-amine (74)**. General procedure B was followed using 2,4-dichloroquinazoline (150 mg, 0.75 mmol) and 1-methylpiperidin-4-amine (112 mg, 0.98 mmol) to obtain **74** as a solid (105 mg, 50%). <sup>1</sup>H NMR (CDCl<sub>3</sub>): δ 7.78-7.69 (m, 3H), 7.48-7.42 (m, 1H), 6.05-6.01 (m, 1H), 4.35-4.28 (m, 1H), 2.91-2.85 (m, 3H), 2.34 (s, 3H), 2.29-2.15 (m, 4H), 1.76-1.63 (m, 2H). MS, m/z (%) = 277 (100) [M + H]<sup>+</sup>, 279 (50).

## ASSOCIATED CONTENT

### Supporting Information

Screening hit data from literature, compound metabolism identification data, plasma exposure values from the *P. berghei* mouse model, dose response curves of selected compounds against *P. falciparum* asexual parasites (3D7 and W2mef), *P. falciparum* gametocytes and HepG2 cytotoxicity. “This material is available free of charge via the Internet at <http://pubs.acs.org>.”

## AUTHOR INFORMATION

### Corresponding Author

\*Dr. Brad E. Sleebs. Phone: +61 3 9345 2718. Email: [sleebs@wehi.edu.au](mailto:sleebs@wehi.edu.au).

## NOTES

The authors declare no conflict of interest with this manuscript.

## ACKNOWLEDGMENTS

This work was funded by the National Health and Medical Research Council of Australia (Program Grant APP1092789), the Australian Cancer Research Foundation, Brian Little Bequest, Victorian State Government Operational Infrastructure Support and Australian Government NHMRC IRIISS. A.F.C. is a Howard Hughes International Scholar and an Australia Fellow of the NHMRC. The authors thank and acknowledge the Australian Red Cross Blood Bank for the provision of fresh red blood cells, without which this research could not have been performed. This work was supported by the Australian Research Council (LP120200557 to V.M.A.). We thank Assoc. Prof. Guillaume Lessene, Dr Andrew Powell and Prof Susan Charman for their helpful discussions, and Halina M. Pietrzak for technical assistance.

## ABBREVIATIONS

APADH, 3-acetylpyridine-adenine dinucleotide (reduced); ART, Artemisinin;  $CL_{int}$ , intrinsic clearance; cLogP, calculated partition co-efficient; CQ, Chloroquine; DHFR, dihydrofolate reductase; DIPEA, diisopropylethylamine; DMEM, Dulbeccos modified eagles medium; DTT, 1,4-dithiothreitol; EDTA, ethylenediaminetetraacetic acid;  $E_H$ , hepatic extraction ratio; FCS, fetal calf serum; GFP, green fluorescent protein; HEPES, (4-(2-hydroxyethyl)-1-piperazineethanesulfonic acid); hERG, human ether-a-go-go-related gene; HPMC, hydroxypropyl-methylcellulose; HTS, high throughput screen; i.p., intraperitoneal injection; LDH, lactate dehydrogenase; MMV, Medicines for Malaria Venture; MTR, MitoTracker Red; MTT, 3-(4,5-dimethylthiazol-2-yl)-2,5-diphenyltetrazolium bromide; NADH, nicotinamide adenine dinucleotide (reduced); NADPH, nicotinamide adenine dinucleotide phosphate (reduced); NAG, N-acetyl glucosamine; PBS, phosphate buffered saline; Pf, *P. falciparum*; p.o., *per os* (oral administration); PSA, polar surface area; Pyr, Pyronaridine; RPMI, Roswell Park Memorial

Institute medium; SAR, structure activity relationship; SI, selectivity index; S<sub>N</sub>Ar, nucleophilic aromatic substitution; SV, saline vehicle; TFA, trifluoroacetic acid; WHO, World Health Organisation.

## REFERENCES

1. World Malaria Report 2016. World Health Organisation, Geneva. <http://www.who.int/malaria/publications/world-malaria-report-2016/report/en/23> (accessed Dec. 23, 2016).
2. Mendis, K.; Sina, B. J.; Marchesini, P.; Carter, R. The neglected burden of *Plasmodium vivax* malaria. *Am. J. Trop. Med. Hyg.* **2001**, *64*, 97-106.
3. Fidock, D. A. Drug discovery: Priming the antimalarial pipeline. *Nature* **2010**, *465*, 297-298.
4. Dondorp, A. M.; Nosten, F.; Yi, P.; Das, D.; Phyo, A. P.; Tarning, J.; Lwin, K. M.; Ariey, F.; Hanpithakpong, W.; Lee, S. J.; Ringwald, P.; Silamut, K.; Imwong, M.; Chotivanich, K.; Lim, P.; Herdman, T.; An, S. S.; Yeung, S.; Singhasivanon, P.; Day, N. P. J.; Lindegardh, N.; Socheat, D.; White, N. J. Artemisinin resistance in *Plasmodium falciparum* malaria. *N. Eng. J. Med.* **2009**, *361*, 455-467.
5. Duffy, S.; Avery, V. M. Identification of inhibitors of *Plasmodium falciparum* gametocyte development. *Malaria J.* **2013**, *12*, 408-408.
6. Meister, S.; Plouffe, D. M.; Kuhlen, K. L.; Bonamy, G. M. C.; Wu, T.; Barnes, S. W.; Bopp, S. E.; Borboa, R.; Bright, a. T.; Che, J.; Cohen, S.; Dharia, N. V.; Gagaring, K.; Gettayacamin, M.; Gordon, P.; Groessler, T.; Kato, N.; Lee, M. C. S.; McNamara, C. W.; Fidock, D. a.; Nagle, A.; Nam, T.-g.; Richmond, W.; Roland, J.; Rottmann, M.; Zhou, B.; Froissard, P.; Glynn, R. J.; Mazier, D.; Sattabongkot, J.; Schultz, P. G.; Tuntland, T.; Walker, J. R.; Zhou, Y.; Chatterjee, A.; Diagana, T. T.; Winzeler, E. a. Imaging of *Plasmodium* liver stages to drive next-generation antimalarial drug discovery. *Science* **2011**, *334*, 1372-1377.

- 1  
2  
3  
4  
5  
6  
7  
8  
9  
10  
11  
12  
13  
14  
15  
16  
17  
18  
19  
20  
21  
22  
23  
24  
25  
26  
27  
28  
29  
30  
31  
32  
33  
34  
35  
36  
37  
38  
39  
40  
41  
42  
43  
44  
45  
46  
47  
48  
49  
50  
51  
52  
53  
54  
55  
56  
57  
58  
59  
60
7. Guiguemde, W. A.; Shelat, A. A.; Bouck, D.; Duffy, S.; Crowther, G. J.; Davis, P. H.; Smithson, D. C.; Connelly, M.; Clark, J.; Zhu, F.; Jimenez-Diaz, M. B.; Martinez, M. S.; Wilson, E. B.; Tripathi, A. K.; Gut, J.; Sharlow, E. R.; Bathurst, I.; Mazouni, F. E.; Fowble, J. W.; Forquer, I.; McGinley, P. L.; Castro, S.; Angulo-Barturen, I.; Ferrer, S.; Rosenthal, P. J.; DeRisi, J. L.; Sullivan, D. J.; Lazo, J. S.; Roos, D. S.; Riscoe, M. K.; Phillips, M. A.; Rathod, P. K.; Van Voorhis, W. C.; Avery, V. M.; Guy, R. K. Chemical genetics of *Plasmodium falciparum*. *Nature* **2010**, *465*, 311-315.
8. Gamo, F.-J.; Sanz, L. M.; Vidal, J.; de Cozar, C.; Alvarez, E.; Lavandera, J.-L.; Vanderwall, D. E.; Green, D. V. S.; Kumar, V.; Hasan, S.; Brown, J. R.; Peishoff, C. E.; Cardon, L. R.; Garcia-Bustos, J. F. Thousands of chemical starting points for antimalarial lead identification. *Nature* **2010**, *465*, 305-310.
9. Plouffe, D.; Brinker, A.; McNamara, C.; Henson, K.; Kato, N.; Kuhlen, K.; Nagle, A.; Adrian, F.; Matzen, J. T.; Anderson, P.; Nam, T. G.; Gray, N. S.; Chatterjee, A.; Janes, J.; Yan, S. F.; Trager, R.; Caldwell, J. S.; Schultz, P. G.; Zhou, Y.; Winzeler, E. A. In silico activity profiling reveals the mechanism of action of antimalarials discovered in a high-throughput screen. *Proc. Natl. Acad. Sci. U.S.A.* **2008**, *105*, 9059-9064.
10. Spangenberg, T.; Burrows, J. N.; Kowalczyk, P.; McDonald, S.; Wells, T. N. C.; Willis, P. The open access malaria box: a drug discovery catalyst for neglected diseases. *PLoS One* **2013**, *8*, e62906.
11. Hansch, C.; Fukunaga, J. Y.; Jow, P. Y. C.; Hynes, J. B. Quantitative structure-activity relation of antimalarial and dihydrofolate reductase inhibition by quinazolines and 5-substituted benzyl-2,4-diaminopyrimidines. *J. Med. Chem.* **1977**, *20*, 96-102.
12. Gonzalez Cabrera, D.; Le Manach, C.; Douelle, F.; Younis, Y.; Feng, T.-S.; Paquet, T.; Nchinda, A. T.; Street, L. J.; Taylor, D.; de Kock, C.; Wiesner, L.; Duffy, S.; White, K. L.; Zabiulla, K. M.; Sambandan, Y.; Bashyam, S.; Waterson, D.; Witty, M. J.; Charman, S. a.; Avery, V. M.; Wittlin, S.; Chibale, K. 2,4-Diaminothienopyrimidines as orally active antimalarial agents. *J. Med. Chem.* **2014**, *57*, 1014-1022.

- 1  
2  
3  
4  
5  
6  
7  
8  
9  
10  
11  
12  
13  
14  
15  
16  
17  
18  
19  
20  
21  
22  
23  
24  
25  
26  
27  
28  
29  
30  
31  
32  
33  
34  
35  
36  
37  
38  
39  
40  
41  
42  
43  
44  
45  
46  
47  
48  
49  
50  
51  
52  
53  
54  
55  
56  
57  
58  
59  
60
13. Hameed P, S.; Solapure, S.; Patil, V.; Henrich, P. P.; Magistrado, P. A.; Bharath, S.; Murugan, K.; Viswanath, P.; Puttur, J.; Srivastava, A.; Bellale, E.; Panduga, V.; Shanbag, G.; Awasthy, D.; Landge, S.; Morayya, S.; Koushik, K.; Saralaya, R.; Raichurkar, A.; Rautela, N.; Roy Choudhury, N.; Ambady, A.; Nandishaiah, R.; Reddy, J.; Prabhakar, K. R.; Menasinakai, S.; Rudrapatna, S.; Chatterji, M.; Jiménez-Díaz, M. B.; Martínez, M. S.; Sanz, L. M.; Coburn-Flynn, O.; Fidock, D. A.; Lukens, A. K.; Wirth, D. F.; Bandodkar, B.; Mukherjee, K.; McLaughlin, R. E.; Waterson, D.; Rosenbrier-Ribeiro, L.; Hickling, K.; Balasubramanian, V.; Warner, P.; Hosagrahara, V.; Dudley, A.; Iyer, P. S.; Narayanan, S.; Kavanagh, S.; Sambandamurthy, V. K. Triaminopyrimidine is a fast-killing and long-acting antimalarial clinical candidate. *Nat. Commun.* **2015**, *6*, 6715.
14. Malmquist, N. a.; Moss, T. a.; Mecheri, S.; Scherf, A.; Fuchter, M. J. Small-molecule histone methyltransferase inhibitors display rapid antimalarial activity against all blood stage forms in *Plasmodium falciparum*. *Proc. Natl. Acad. Sci. U.S.A.* **2012**, *109*, 16708-16713.
15. Elslager, E. F.; Hess, C.; Johnson, J.; Ortwine, D.; Chu, V.; Werbel, L. M. Synthesis and antimalarial effects of N2-aryl-N4-[(dialkylamino)alkyl]- and N4-aryl-N2-[(dialkylamino)alkyl]-2,4-quinazolinediamines. *J. Med. Chem.* **1981**, *24*, 127-140.
16. N2-(3,4-dichlorophenyl)-N4-[2-(1-methyl-2-pyrrolidiny)-ethyl]-2,4-quinazolinediamine (compound 19 from reference 15) was the most promising compound from this study. Compound 19 is structurally related to the lead compounds **53-56** described in this article.
17. A direct comparison of the asexual stage activity of compounds generated in this article were compared to compounds described in the original HT screening sets (references 7 and 9) in Table S1.
18. Makler, M. T.; Hinrichs, D. J. Measurement of the lactate dehydrogenase activity of *Plasmodium falciparum* as an assessment of parasitemia. *Am. J. Trop. Med. Hyg.* **1993**, *48*, 205-210.
19. Peterson, L. A. Reactive metabolites in the biotransformation of molecules containing a furan ring. *Chem. Res. Toxicol.* **2013**, *26*, 6-25.

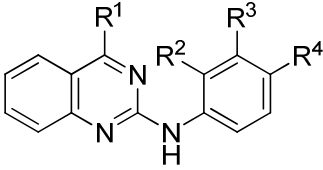
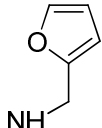
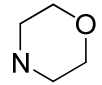
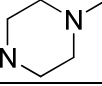
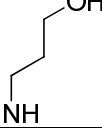
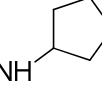
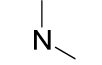
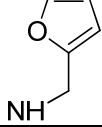
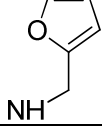
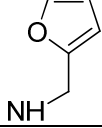
- 1  
2  
3  
4  
5  
6  
7  
8  
9  
10  
11  
12  
13  
14  
15  
16  
17  
18  
19  
20  
21  
22  
23  
24  
25  
26  
27  
28  
29  
30  
31  
32  
33  
34  
35  
36  
37  
38  
39  
40  
41  
42  
43  
44  
45  
46  
47  
48  
49  
50  
51  
52  
53  
54  
55  
56  
57  
58  
59  
60
20. Fujita, T.; Suzuoki, Z. Enzymatic studies on the metabolism of the tetrahydrofurfuryl mercaptan moiety of thiamine tetrahydrofurfuryl disulfide: III. Oxidative cleavage of the tetrahydrofuran moiety. *J. Biochem.* **1973**, *74*, 733-738.
21. Rietjens, I. M. C. M.; Vervoort, J. Bioactivation of 4-fluorinated anilines to benzoquinoneimines as primary reaction products. *Chem.-Biol. Interactions* **1991**, *77*, 263-281.
22. Li, X.; Kamenecka, T. M.; Cameron, M. D. Bioactivation of the epidermal growth factor receptor inhibitor Gefitinib: Implications for pulmonary and hepatic toxicities. *Chem. Res. Toxicol.* **2009**, *22*, 1736-1742.
23. Cnubben, N. H. P.; Vervoort, J.; Boersma, M. G.; Rietjens, I. M. C. M. The effect of varying halogen substituent patterns on the cytochrome P450 catalysed dehalogenation of 4-halogenated anilines to 4-aminophenol metabolites. *Biochem. Pharmacol.* **1995**, *49*, 1235-1248.
24. Cowman, A. F.; Galatis, D.; Thompson, J. K. Selection for mefloquine resistance in *Plasmodium falciparum* is linked to amplification of the pfmdr1 gene and cross-resistance to halofantrine and quinine. *Proc. Natl. Acad. Sci. U.S.A.* **1994**, *91*, 1143-1147.
25. Dogovski, C.; Xie, S. C.; Burgio, G.; Bridgford, J.; Mok, S.; McCaw, J. M.; Chotivanich, K.; Kenny, S.; Gnadig, N.; Straimer, J.; Bozdech, Z.; Fidock, D. A.; Simpson, J. A.; Dondorp, A. M.; Foote, S.; Klonis, N.; Tilley, L. Targeting the cell stress response of *Plasmodium falciparum* to overcome artemisinin resistance. *PLoS Biol.* **2015**, *13*, e1002132.
26. Azevedo, M. F.; Nie, C. Q.; Elsworth, B.; Charnaud, S. C.; Sanders, P. R.; Crabb, B. S.; Gilson, P. R. *Plasmodium falciparum* transfected with ultra bright NanoLuc luciferase offers high sensitivity detection for the screening of growth and cellular trafficking inhibitors. *PLoS One* **2014**, *9*, e112571.
27. Fidock, D. a.; Rosenthal, P. J.; Croft, S. L.; Brun, R.; Nwaka, S. Antimalarial drug discovery: efficacy models for compound screening. *Nat. Rev. Drug Discovery* **2004**, *3*, 509-520.
28. Wang, S.-B.; Cui, M.-T.; Wang, X.-F.; Ohkoshi, E.; Goto, M.; Yang, D.-X.; Li, L.; Yuan, S.; Morris-Natschke, S. L.; Lee, K.-H.; Xie, L. Synthesis, biological evaluation, and physicochemical

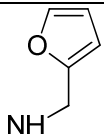
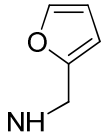
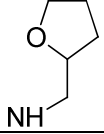
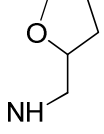
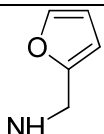
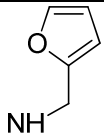
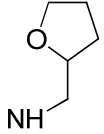
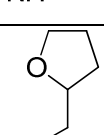
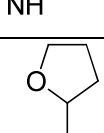
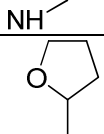
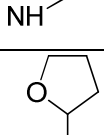
- 1  
2 property assessment of 4-substituted 2-phenylaminoquinazolines as Mer tyrosine kinase inhibitors.  
3  
4 *Bioorg. Med. Chem.* **2016**, *24*, 3083-3092.
- 5  
6  
7 29. Michellys, P.-Y.; Chen, B.; Jiang, T.; Jin, Y.; Lu, W.; Marsilje, T. H.; Pei, W.; Uno, T.; Zhu,  
8  
9 X.; Wu, B.; Nguyen, T. N.; Bursulaya, B.; Lee, C.; Li, N.; Kim, S.; Tuntland, T.; Liu, B.; Sun, F.;  
10  
11 Steffy, A.; Hood, T. Design and synthesis of novel selective anaplastic lymphoma kinase inhibitors.  
12  
13 *Bioorg. Med. Chem. Lett.* **2016**, *26*, 1090-1096.
- 14  
15  
16 30. Lazarus, M. B.; Shokat, K. M. Discovery and structure of a new inhibitor scaffold of the  
17  
18 autophagy initiating kinase ULK1. *Bioorg. Med. Chem.* **2015**, *23*, 5483-5488.
- 19  
20  
21 31. Zhou, H.-J.; Wang, J.; Yao, B.; Wong, S.; Djakovic, S.; Kumar, B.; Rice, J.; Valle, E.; Soriano,  
22  
23 F.; Menon, M.-K.; Madriaga, A.; Kiss von Soly, S.; Kumar, A.; Parlati, F.; Yakes, F. M.; Shawver, L.;  
24  
25 Le Moigne, R.; Anderson, D. J.; Rolfe, M.; Wustrow, D. Discovery of a first-in-class, potent, selective,  
26  
27 and orally bioavailable inhibitor of the p97 AAA ATPase (CB-5083). *J. Med. Chem.* **2015**, *58*, 9480-  
28  
29 9497.
- 30  
31  
32 32. Chou, T.-F.; Li, K.; Frankowski, K. J.; Schoenen, F. J.; Deshaies, R. J. Structure-activity  
33  
34 relationship study reveals ML240 and ML241 as potent and selective inhibitors of p97 ATPase.  
35  
36 *ChemMedChem* **2013**, *8*, 297-312.
- 37  
38  
39 33. Ife, R. J.; Brown, T. H.; Blurton, P.; Keeling, D. J.; Leach, C. A.; Meeson, M. L.; Parsons, M.  
40  
41 E.; Theobald, C. J. Reversible inhibitors of the gastric (H<sup>+</sup>/K<sup>+</sup>)-ATPase. 5. Substituted 2,4-  
42  
43 diaminoquinazolines and thienopyrimidines. *J. Med. Chem.* **1995**, *38*, 2763-2773.
- 44  
45  
46 34. Deng, X.; Guo, L.; Xu, L.; Zhen, X.; Yu, K.; Zhao, W.; Fu, W. Discovery of novel potent and  
47  
48 selective ligands for 5-HT<sub>2A</sub> receptor with quinazoline scaffold. *Bioorg. Med. Chem.* **2015**, *25*, 3970-  
49  
50 3974.
- 51  
52  
53 35. Pham, T.-A. N.; Yang, Z.; Fang, Y.; Luo, J.; Lee, J.; Park, H. Synthesis and biological  
54  
55 evaluation of novel 2,4-disubstituted quinazoline analogues as GPR119 agonists. *Bioorg. Med. Chem.*  
56  
57 **2013**, *21*, 1349-1356.
- 58  
59  
60

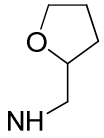
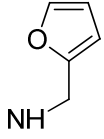
- 1  
2  
3  
4  
5  
6  
7  
8  
9  
10  
11  
12  
13  
14  
15  
16  
17  
18  
19  
20  
21  
22  
23  
24  
25  
26  
27  
28  
29  
30  
31  
32  
33  
34  
35  
36  
37  
38  
39  
40  
41  
42  
43  
44  
45  
46  
47  
48  
49  
50  
51  
52  
53  
54  
55  
56  
57  
58  
59  
60
36. Rueeger, H.; Rigollier, P.; Yamaguchi, Y.; Schmidlin, T.; Schilling, W.; Criscione, L.; Whitebread, S.; Chiesi, M.; Walker, M. W.; Dhanoa, D.; Islam, I.; Zhang, J.; Gluchowski, C. Design, synthesis and SAR of a series of 2-substituted 4-amino-quinazoline neuropeptide Y Y5 receptor antagonists. *Bioorg. Med. Chem. Lett.* **2000**, *10*, 1175-1179.
37. Trager, W.; Jensen, J. B. Human malaria parasites in continuous culture. *Science* **1976**, *193*, 673-675.
38. Pingaew, R.; Mandi, P.; Nantasenamat, C.; Prachayasittikul, S.; Ruchirawat, S.; Prachayasittikul, V. Design, synthesis and molecular docking studies of novel N-benzenesulfonyl-1,2,3,4-tetrahydroisoquinoline-based triazoles with potential anticancer activity. *Euro. J. Med. Chem.* **2014**, *81*, 192-203.
39. Duffy, S.; Loganathan, S.; Holleran, J. P.; Avery, V. M. Large-scale production of *Plasmodium falciparum* gametocytes for malaria drug discovery. *Nat. Protoc.* **2016**, *11*, 976-992.
40. Bevan, C. D.; Lloyd, R. S. A high-throughput screening method for the determination of aqueous drug solubility using laser nephelometry in microtiter plates. *Anal. Chem.* **2000**, *72*, 1781-1787.
41. Obach, R. S. Prediction of human clearance of twenty-nine drugs from hepatic microsomal intrinsic clearance data: an examination of in vitro half-life approach and non-specific binding to microsomes. *Drug Metab. Dispos.* **1999**, *27*, 1350-1359.
42. Ring, B. J.; Chien, J. Y.; Adkison, K. K.; Jones, H. M.; Rowland, M.; Jones, R. D.; Yates, J. W. T.; Ku, M. S.; Gibson, C. R.; He, H.; Vuppugalla, R.; Marathe, P.; Fischer, V.; Dutta, S.; Sinha, V. K.; Björnsson, T.; Lavé, T.; Poulin, P. PhRMA CPCDC initiative on predictive models of human pharmacokinetics, part 3: Comparative assessment of prediction methods of human clearance. *J. Pharm. Sci.* **2011**, *100*, 4090-4110.
43. Calculator Plugins were used for structure property prediction and calculation, MarvinSketch 6.0.6., 2013, ChemAxon (<http://www.chemaxon.com>).

## TABLES AND FIGURES

**Table 1.** Activity of early generation analogues against *P. falciparum* parasites.

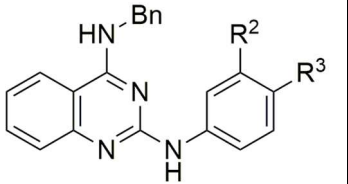
Cmpd					Pf parasite EC <sub>50</sub> (SD) nM <sup>a</sup>	HepG2 EC <sub>50</sub> (SD) <sub>b</sub> μM	SI <sub>c</sub>	PSA (Å <sup>2</sup> ) <sub>d</sub>	cLogP <sub>d</sub>	Lip E
	R <sup>1</sup>	R <sup>2</sup>	R <sup>3</sup>	R <sup>4</sup>						
1		H	H	OCH <sub>3</sub>	124 (32)	2.5 (1.4)	20	72	4.2	2.7
2		H	H	OCH <sub>3</sub>	7700 (1900)	25.6 (11.9)	3	60	3.9	1.2
3		H	H	OCH <sub>3</sub>	1800 (400)	>40	>2 2	55	3.9	1.8
4		H	H	OCH <sub>3</sub>	329 (100)	15.9 (3.2)	59	79	2.8	3.7
5		H	-OCH <sub>2</sub> O-		114 (46)	7.8 (1.7)	69	60	4.6	2.3
6	NHCH <sub>3</sub>	H	H	OCH <sub>3</sub>	155 (79)	26.1 (19.7)	16 8	59	3.5	3.3
7	NHCH <sub>3</sub>	H	H	F	136 (110)	16.2 (5.8)	11 9	50	3.8	3.1
8		H	H	F	418 (70)	20.1 (1.8)	48	40	4.4	2.0
9		H	H	CH <sub>3</sub>	109 (14)	5.9 (0.8)	54	63	4.9	2.1
10		H	H	Br	125 (23)	19.0 (15.7)	15 3	63	5.2	1.7
11		H	H	Cl	113 (13)	7.4 (1.3)	71	63	5.0	1.9

12		H	H	F	112 (30)	4.9 (1.9)	43	63	4.5	2.5
14		H	Cl	H	134 (35)	5.0 (3.9)	37	63	5.0	1.9
15		H	F	H	144 (65)	8.6 (11.7)	39	59	4.2	2.5
16		F	H	H	317 (88)	21.3 (3.6)	75	59	4.2	1.9
17		H	H	CO <sub>2</sub> CH <sub>3</sub>	574 (83)	33.5 (21.3)	58	89	4.4	2.6
18		H	H	CH(CH <sub>3</sub> )OH	702 (331)	12.6 (5.3)	36	83	4.0	2.3
19		H	H	C(O)NH <sub>2</sub>	691 (29)	34.6 (7.6)	50	102	2.9	1.8
20		H	H	C(O)NH <sub>2</sub>	569 (265)	20.0 (1.0)	35	88	3.3	2.2
21		H	H	NHAc	274 (11)	38.3 (2.3)	14 0	88	3.3	3.3
22		H	-OCH <sub>2</sub> O-		169 (21)	8.6 (1.1)	51	78	3.7	3.1
23		H	OCH 3	H	230 (480)	7.7 (2.1)	33	68	3.9	2.7
24		OCH 3	H	H	526 (304)	24.5 (5.0)	47	68	3.9	2.4

25		OCH 3	H	OCH <sub>3</sub>	1100 (500)	15.8 (4.2)	19	102	2.9	3.1
26		OCH 3	OCH 3	H	1300 (640)	20.1 (1.3)	64	81	4.1	1.8

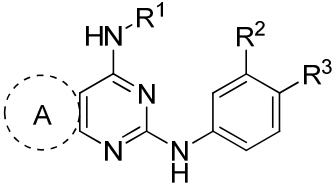
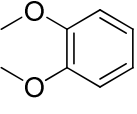
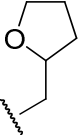
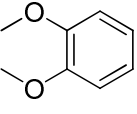
<sup>a</sup> EC<sub>50</sub> data represents means and SDs for three or more independent experiments measuring LDH activity of *P. falciparum* 3D7 parasites following exposure to compounds in a 10-point dilution series for 72 h. Chloroquine EC<sub>50</sub> 23 (10) nM; Artemisinin EC<sub>50</sub> 8 (7) nM. <sup>b</sup> EC<sub>50</sub> data represents means and SDs for 3 or more HepG2 growth inhibition experiments in a 10-point dilution series over 48 h. Cell Titer-Glo was used to quantify cell growth inhibition. <sup>c</sup> Selectivity index – ratio between *P. falciparum* 3D7 viability and HepG2 cytotoxicity. <sup>d</sup> Calculated using ChemAxon software.<sup>43</sup>

**Table 2.** *P. falciparum* parasite activity and cytotoxicity of 4-N-benzyl 2-anilino analogues.

Cmpd			Pf parasite EC <sub>50</sub> (SD) nM <sup>a</sup>	HepG2 EC <sub>50</sub> (SD) μM <sup>b</sup>	SI <sup>c</sup>	PSA (Å <sup>2</sup> ) <sub>d</sub>	cLogP <sub>d</sub>	LigE
	R <sup>2</sup>	R <sup>3</sup>						
<b>27</b>	H	OCH <sub>3</sub>	264 (89)	8.5 (8.6)	32	32	5.2	1.4
<b>28</b>	H	OCH <sub>2</sub> CH <sub>3</sub>	159 (148)	4.5 (3.6)	29	84	5.3	1.5
<b>29</b>	H	F	77 (18)	5.1 (4.2)	67	50	5.5	1.6
<b>30</b>	H	CF <sub>3</sub>	105 (101)	6.4 (1.3)	155	62	6.2	0.8
<b>31</b>	Cl	Br	137 (79)	2.9 (1.4)	40	50	6.7	0.2
<b>32</b>	Cl	F	56 (51)	6.3 (0.3)	114	50	6.1	1.2
<b>33</b>	F	Cl	121 (87)	6.6 (1.1)	55	50	6.1	0.8
<b>34</b>	(N)	CF <sub>3</sub>	102 (88)	8.9 (3.2)	87	63	5.4	1.6

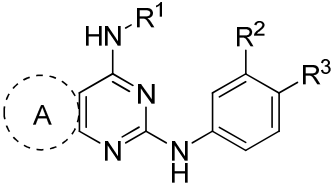
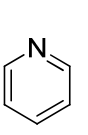
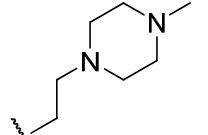
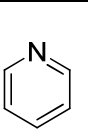
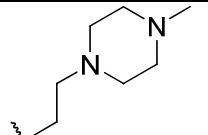
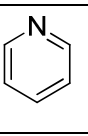
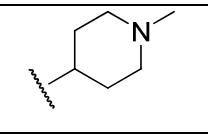
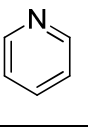
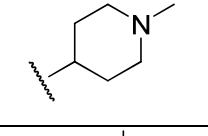
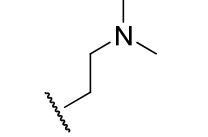
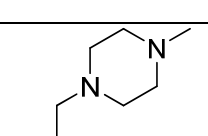
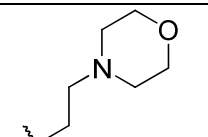
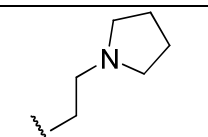
<sup>a</sup> EC<sub>50</sub> data represents means and SDs for three or more independent experiments measuring LDH activity of *P. falciparum* 3D7 parasites following exposure to compounds in a 10-point dilution series for 72 h. Chloroquine EC<sub>50</sub> 23 (10) nM; Artemisinin EC<sub>50</sub> 8 (7) nM. <sup>b</sup> EC<sub>50</sub> data represents means and SDs for 3 or more HepG2 growth inhibition experiments in a 10-point dilution series over 48 h. Cell Titer-Glo was used to quantify cell growth inhibition. <sup>c</sup> Selectivity index – ratio between *P. falciparum* 3D7 viability and HepG2 cytotoxicity. <sup>d</sup> Calculated using ChemAxon software.<sup>43</sup>

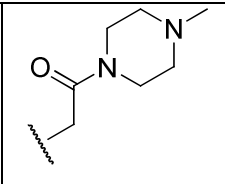
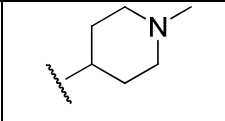
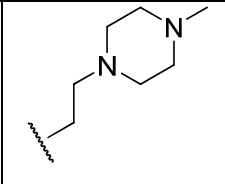
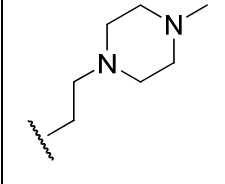
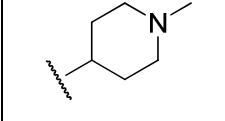
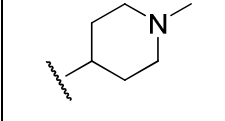
**Table 3.** Activity of compounds against *P. falciparum* parasites.

					Pf parasite EC <sub>50</sub> (SD) nM <sup>a</sup>	HepG2 EC <sub>50</sub> (SD) μM <sup>b</sup>	SI <sup>c</sup>	PSA (Å <sup>2</sup> ) <sup>d</sup>	cLogP <sup>d</sup>	LigE
<b>29</b>	Ar	Bn	H	F	77 (18)	5.1 (4.2)	67	50	5.5	1.6
<b>35</b>			H	F	57 (16)	5.5 (1.8)	96	78	3.9	3.3
<b>36</b>		Bn	H	F	41 (14)	2.8 (1.2)	109	68	5.2	2.2
<b>37</b>		Bn	H	F	539 (349)	17.8 (4.4)	33	63	4.6	1.7
<b>38</b>		Bn	H	F	636 (667)	12.4 (14.0)	8	63	4.6	1.6
<b>39</b>		Bn	H	F	57 (42)	18.2 (7.7)	320	63	4.6	2.6
<b>40</b>		Bn	H	F	866 (642)	18.7 (4.9)	118	50	5.4	0.7
<b>41</b>		Bn	H	F	1200 (200)	9.0 (4.0)	7	68	3.9	2.0
<b>42</b>		Bn	H	F	7600 (400)	26.0 (3.3)	3	68	3.9	1.2

<sup>a</sup> EC<sub>50</sub> data represents means and SDs for three or more independent experiments measuring LDH activity of *P. falciparum* 3D7 parasites following exposure to compounds in a 10-point dilution series for 72 h. Chloroquine EC<sub>50</sub> 23 (10) nM; Artemisinin EC<sub>50</sub> 8 (7) nM. <sup>b</sup> EC<sub>50</sub> data represents means SDs for 3 or more HepG2 growth inhibition experiments in a 10-point dilution series over 48 h. Cell Titer-Glo was used to quantify cell growth inhibition. <sup>c</sup> Selectivity index – ratio between *P. falciparum* 3D7 viability and HepG2 cytotoxicity. <sup>d</sup> Calculated using ChemAxon software.<sup>43</sup>

**Table 4.** Activity of 4-substituted analogues against *P. falciparum* parasites.

Cmpd					Pf parasite EC <sub>50</sub> (SD) nM <sup>a</sup>	HepG2 EC <sub>50</sub> (SD) μM <sup>b</sup>	SI <sup>c</sup>	PSA (Å <sup>2</sup> ) <sup>d</sup>	cLogP <sub>d</sub>	LigE
	A	R <sup>1</sup>	R <sup>2</sup>	R <sup>3</sup>						
43			Cl	F	110 (12)	8.9 (2.1)	80	70	3.4	3.6
44			F	Cl	128 (23)	12.3 (2.6)	96	70	3.4	3.5
45			Cl	F	134 (51)	11.5 (6.2)	86	67	3.6	3.3
46			F	Cl	283 (141)	11.1 (0.3)	39	67	3.6	2.9
47	Ar		H	F	104 (64)	27.9 (3.0)	267	54	3.8	3.2
48	Ar		H	F	42 (19)	15.3 (5.0)	362	58	3.6	3.8
49	Ar		H	F	118 (51)	30.1 (4.1)	256	62	3.6	3.3
50	Ar		H	F	77 (23)	26.5 (4.1)	343	54	4.2	2.9

51	Ar		H	F	64 (44)	30.4 (8.4)	473	73	2.7	4.5
52	Ar		H	F	51 (31)	11.5 (1.4)	227	54	3.8	3.5
53	Ar		Cl	F	26 (9)	6.1 (2.6)	240	58	4.2	3.4
54	Ar		F	Cl	27 (9)	7.5 (5.1)	275	58	4.2	3.4
55	Ar		Cl	F	35 (13)	5.1 (3.9)	145	54	4.4	3.1
56	Ar		F	Cl	28 (9)	5.1 (2.4)	179	54	4.4	3.2

<sup>a</sup> EC<sub>50</sub> data represents means and SDs for three or more independent experiments measuring LDH activity of *P. falciparum* 3D7 parasites following exposure to compounds in a 10-point dilution series for 72 h. Chloroquine EC<sub>50</sub> 23 (10) nM; Artemisinin EC<sub>50</sub> 8 (7) nM. <sup>b</sup> EC<sub>50</sub> data represents means and SDs for 3 or more HepG2 growth inhibition experiments in a 10-point dilution series over 48 h. Cell Titer-Glo was used to quantify cell growth inhibition. <sup>c</sup> Selectivity index – ratio between *P. falciparum* 3D7 viability and HepG2 cytotoxicity. <sup>d</sup> Calculated using ChemAxon software.<sup>43</sup>

**Table 5.** Physicochemical and metabolism properties of selected compounds.

Cmpn d	Solubility		Human liver microsomes			Mouse liver microsomes			PS A (Å <sup>2</sup> ) c	cLog P <sup>c</sup>
	pH 6.5 (μM) ) <sup>a</sup>	pH 2.0 (μM) ) <sup>a</sup>	half life (min )	<i>in vitro</i> CL <sub>int</sub> (μL/min/m g protein)	predicte d E <sub>H</sub> <sup>b</sup>	half life (min )	<i>in vitro</i> CL <sub>int</sub> (μL/min/m g protein)	predicte d E <sub>H</sub> <sup>b</sup>		
<b>27</b>	1.6 - 3.1	25 - 50	65	27	0.51	14	123	0.73	59	5.2
<b>35</b>	3.1 - 6.3	25 - 50	64	27	0.52	24	72	0.61	78	3.9
<b>36</b>	1.6 - 3.1	1.6 - 3.1	>247	<7	<0.22	49	35	0.43	68	5.2
<b>53</b>	11.3 - 23	>90	>255	<7	<0.22	30	57	0.55	58	4.2
<b>54</b>	10.9 - 22	>90	77	23	0.47	47	37	0.44	58	4.2
<b>55</b>	11.3 - 23	>90	>255	<7	<0.22	149	12	0.20	54	4.4
<b>56</b>	4.2 - 8.4	>90	181	10	0.28	192	9	0.16	54	4.4

<sup>a</sup> Estimated by nephelometry. <sup>b</sup> Predicted hepatic extraction (E<sub>H</sub>) ratio based on *in vitro* intrinsic clearance (CL<sub>int</sub>). <sup>c</sup> Calculated using ChemAxon software.<sup>43</sup>

**Table 6.** Comparison of 3D7 and multidrug resistant *P. falciparum* activity of selected compounds.

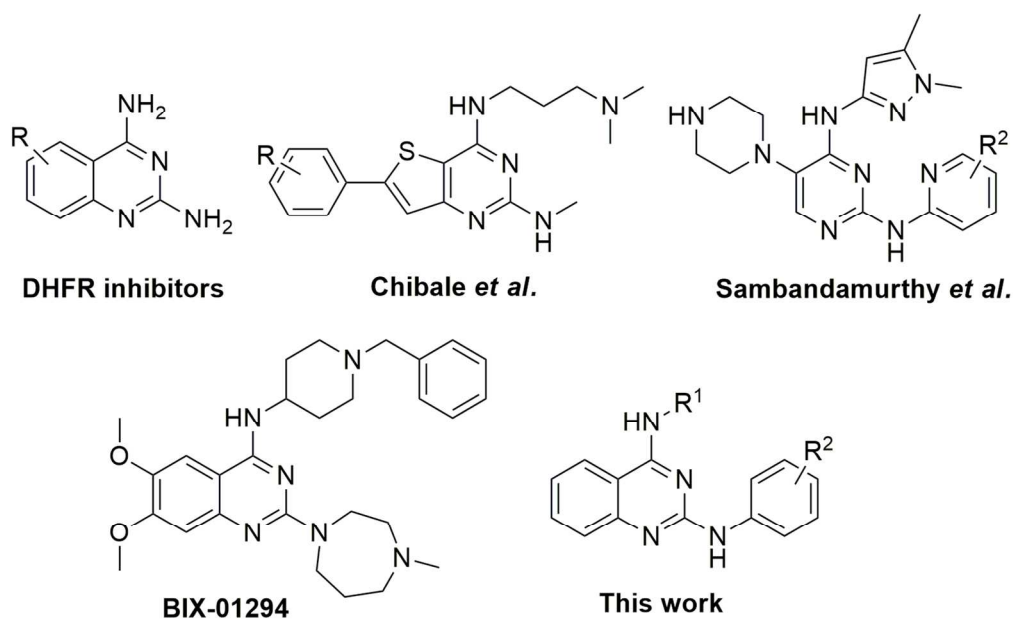
Cmpnd	3D7 EC <sub>50</sub> (SD) nM <sup>a</sup>	W2mef EC <sub>50</sub> (SD) nM <sup>b</sup>
<b>31</b>	137 (79)	128 (88)
<b>32</b>	56 (51)	80 (12)
<b>33</b>	121 (87)	75 (17)
<b>48</b>	42 (19)	122 (4)
<b>53</b>	26 (9)	49 (24)
<b>54</b>	27 (9)	57 (26)
<b>55</b>	35 (13)	54 (23)
<b>56</b>	28 (9)	61 (29)
<b>CQ</b>	23 (10)	250 (92)
<b>ART</b>	8 (7)	6 (2)

<sup>a</sup> Data taken from Tables 1-3 for comparison. <sup>b</sup> EC<sub>50</sub> data represents means and SDs for three or more experiments measuring LDH activity of multi-drug resistant *P. falciparum* W2mef parasites following exposure to compounds in 10-point dilution series for 72 h. CQ = chloroquine; ART = artesunate.

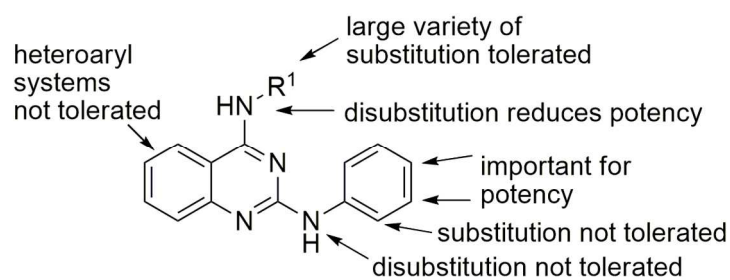
**Table 7.** *P. falciparum* NF54 gametocyte activity of compounds **53-56**.

Cmpnd	Ring stage	Early stage I-III	Late stage IV-V
	EC <sub>50</sub> (SD) nM <sup>a</sup>	EC <sub>50</sub> (SD) nM <sup>a</sup>	EC <sub>50</sub> (SD) nM <sup>a</sup>
<b>53</b>	179 (36)	326 (54)	3000 (100)
<b>54</b>	207 (10)	453 (16)	4000 (100)
<b>55</b>	223 (20)	515 (15)	3700 (200)
<b>56</b>	220 (2)	554 (20)	2700 (300)
<b>CQ</b>	20 (14)	59 (3)	>40000
<b>ART</b>	3 (3)	3 (2)	8 (1)
<b>Pyr</b>	16 (7)	25 (2)	1400 (100)

<sup>a</sup> EC<sub>50</sub> data represents means and SDs for three or more experiments following exposure to compounds in 21-point dilution series. Synchronous *P. falciparum* NF54 ring stage gametocytes (day 0) were treated with compound for 24 h for ring stage, day 2 gametocytes for 48 h for early stage, and day 8 gametocytes for 48 h for late stage EC<sub>50</sub> determination. Parasitemia was quantified by a high content imaging algorithm measuring morphology of NF54 parasites expressing the gametocyte specific protein, pfs16-GFP and MitoTracker Red, as a viability marker. CQ = chloroquine; ART = Artesunate; Pyr = Pyronaridine.



23 **Figure 1.** The 2-anilino-4-amino-quinazoline scaffold – the focus of this study; and related scaffolds  
24 with antimalarial activity previously described by other groups in literature.  
25  
26  
27  
28  
29  
30  
31  
32  
33  
34  
35



46 **Figure 2.** Summary of structure activity relationship.  
47  
48  
49  
50  
51  
52  
53  
54  
55  
56  
57  
58  
59  
60

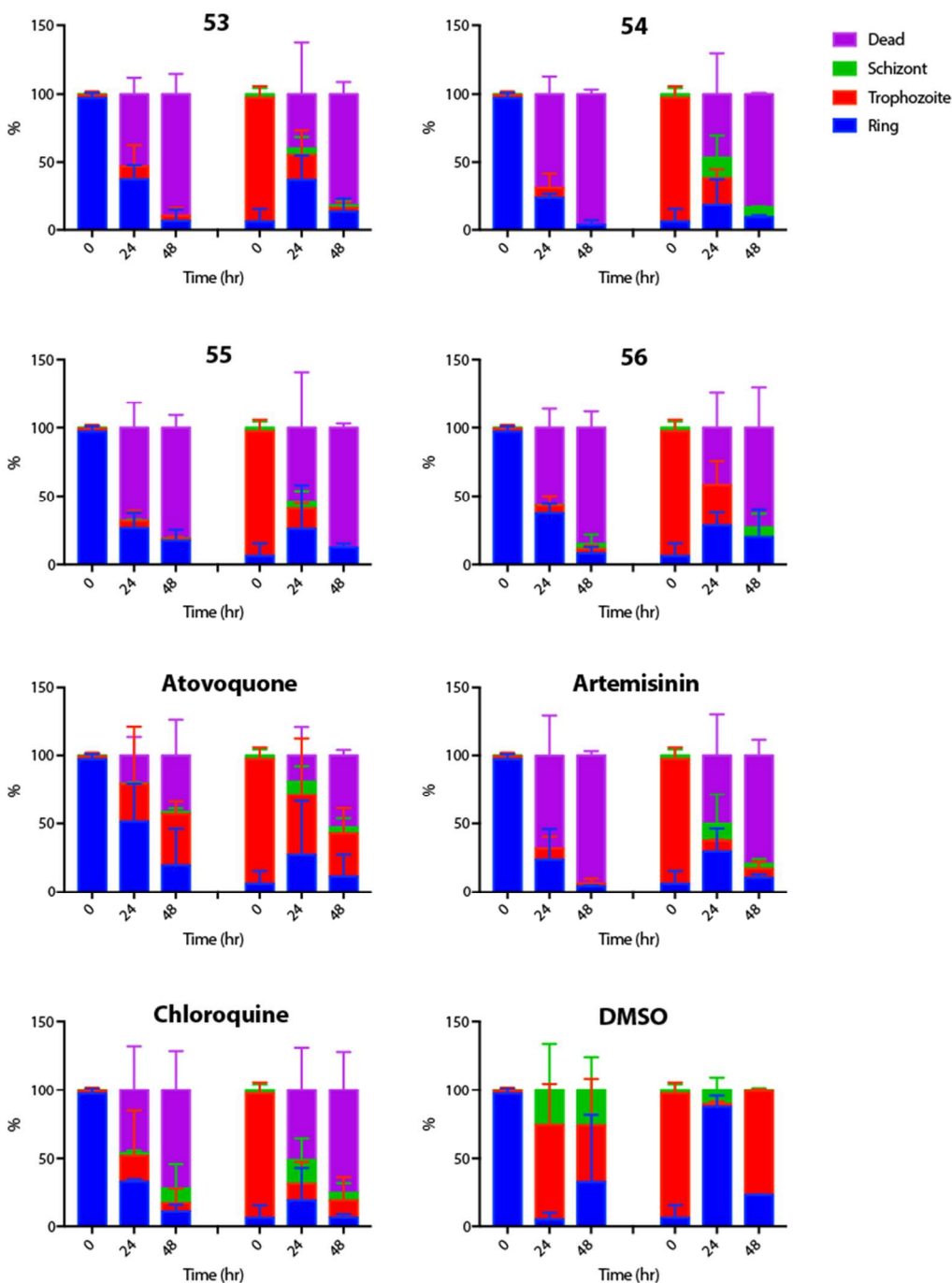


**Figure 3.** Compounds **53-56** arrest parasites at ring stage. Wildtype 3D7 parasites at the stages indicated were treated with 10 times  $EC_{50}$  of the compounds shown and parasites visible by Giemsa smears were counted at each time point listed and classified as either ring, trophozoite, schizont or dead (pyknotic). Parasites treated at rings (blue) are shown in left hand bars, parasites treated at trophozoites (red) are shown in right hand bars. Results represent mean values for 1000 cells counted for three biological replicates. Error bars represent SD.

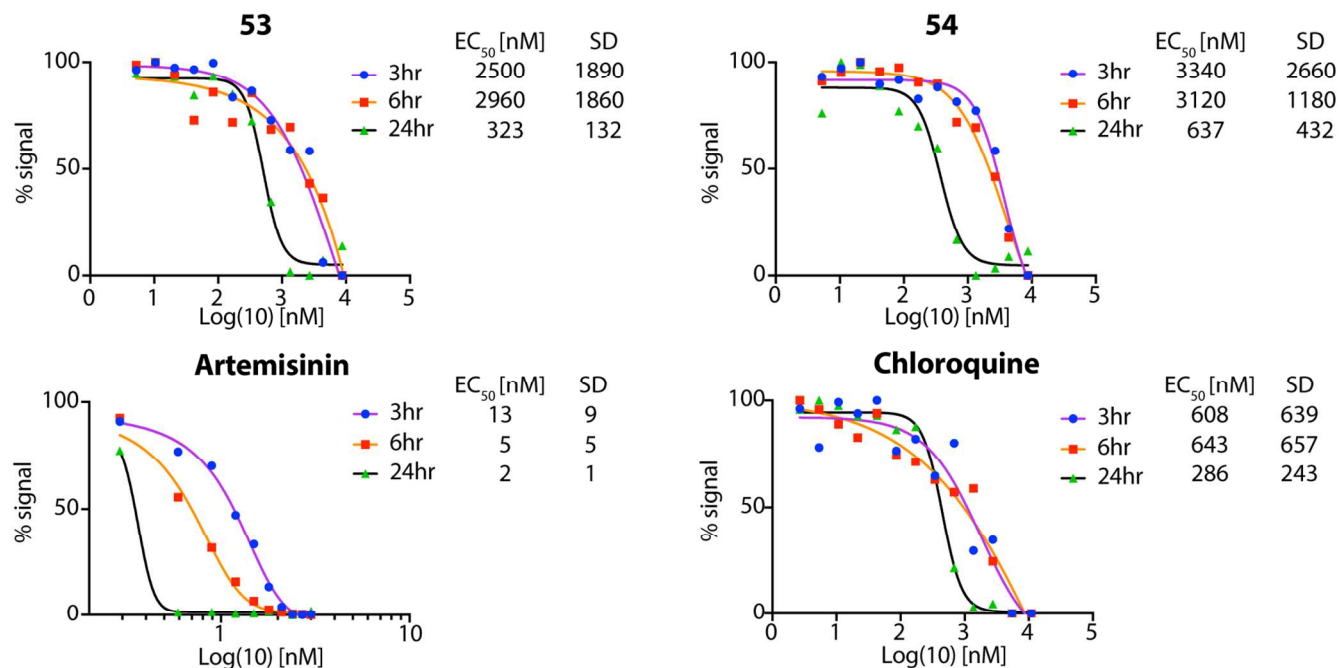


**Figure 4.** Compounds **53** and **54** are active over 24 h. 3D7 parasites expressing nanoluciferase were treated for increasing lengths of time with a dilution series of compounds **53** and **54**, artemisinin, or chloroquine (controls) before washing out the drug and allowing parasites to continue growing for a total time of 24 h. Parasite viability was determined by plotting the normalized total nanoluciferase signal for each treatment, and EC<sub>50</sub> values were calculated for each time point using GraphPad PRISM software. Data are representative of results obtained from five biological replicates completed in duplicate. Mean EC<sub>50</sub> and SD are shown for each treatment condition. **53** and **54** are active over 24 h. Control compound artemisinin was more rapidly acting within this time period, whereas chloroquine acted over a similar timeframe but with lower EC<sub>50</sub>. The single graphs shown are representative of 9 to 13 biological replicates, each of 2 technical replicates.

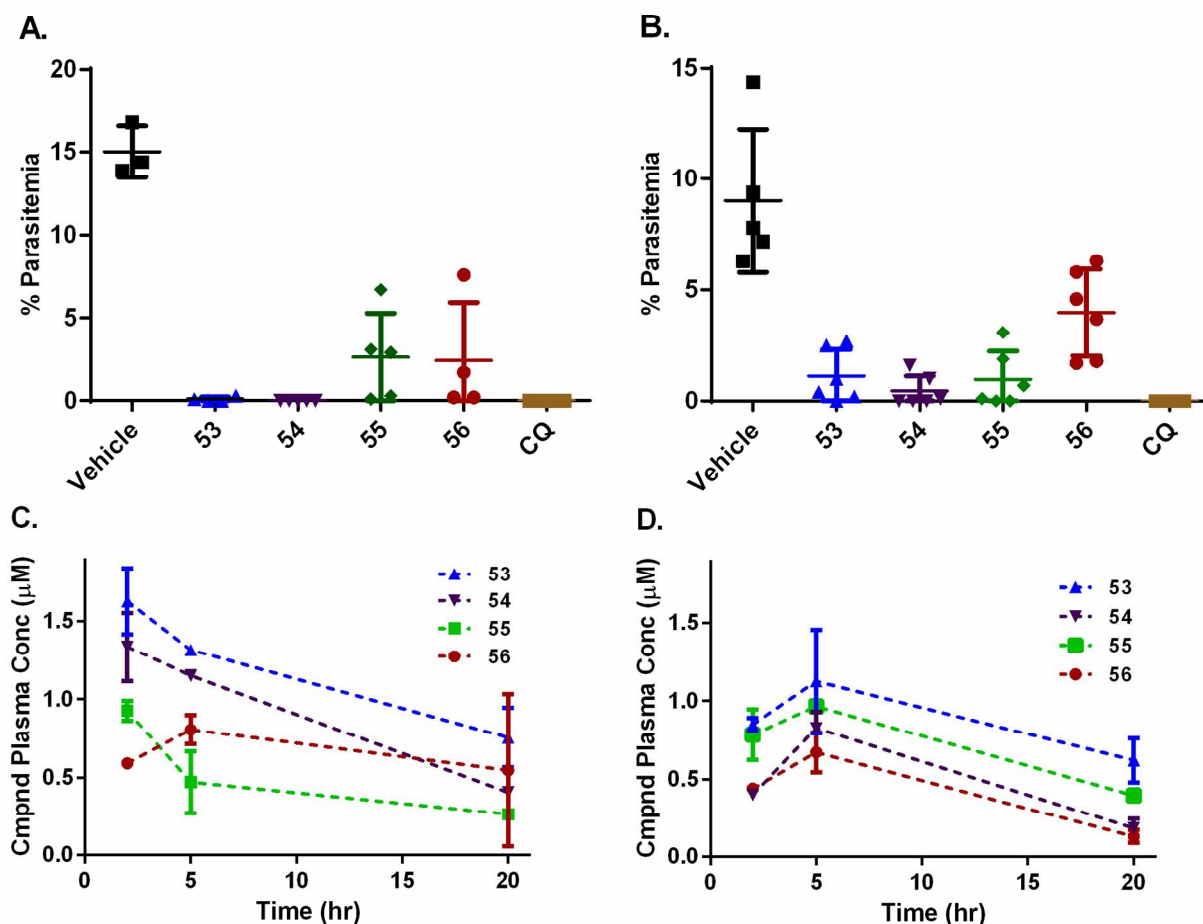
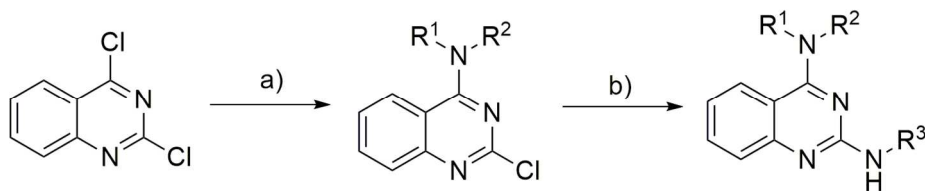


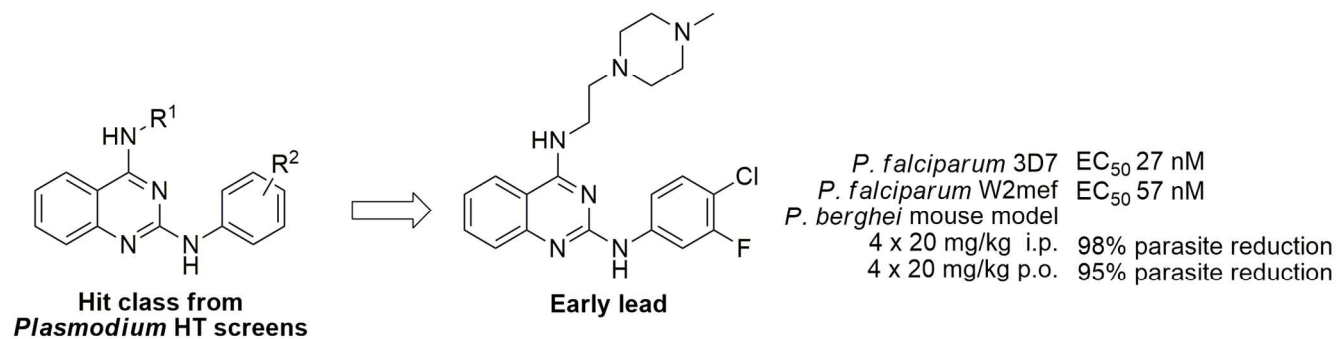
**Figure 5.** Evaluation of compounds **53-56** in a Peter's 4 day *P. berghei* mouse model. To infect mice, *P. berghei* parasites ( $2 \times 10^7$  parasites) were injected into the tail vein. Drug was then administered 4 h after infection (day 0) and then on day 1, 2 and 3. On the fourth day blood smears were taken and parasitemia evaluated. Data is an average for  $n=6$  mice. A) Compounds were dosed 20 mg/kg by i.p. using a solutol/saline vehicle. B) Compounds were dosed 20 mg/kg by p.o. using a HPMC-SV vehicle. For both A) and B), chloroquine (CQ) (10 mg/kg) was used as a positive control; unpaired t test (vs vehicle), P value for all compounds  $<0.0001$ ; a ANOVA test (between each compound independently), no statistical significance; error bars represent SD. C) Plasma exposure levels of the compounds in mice on day 0 of the Peter's 4 day model dosed by i.p. D) Plasma exposure levels of the compounds in mice on day 0 of the Peter's 4 day model dosed by p.o. For both C) and D), data is an average of  $n=2$  mice; error bars represent SD.

**Scheme 1.** General pathway to synthesize quinazoline analogues.<sup>a</sup>



<sup>a</sup> Reagents and conditions: a)  $R^1R^2-NH$ , 20°C, 20 h; b)  $R^3-NH_2$ , iPrOH, TFA, 120 °C,  $\mu W$ , 15 min.

## TABLE OF CONTENTS GRAPHIC



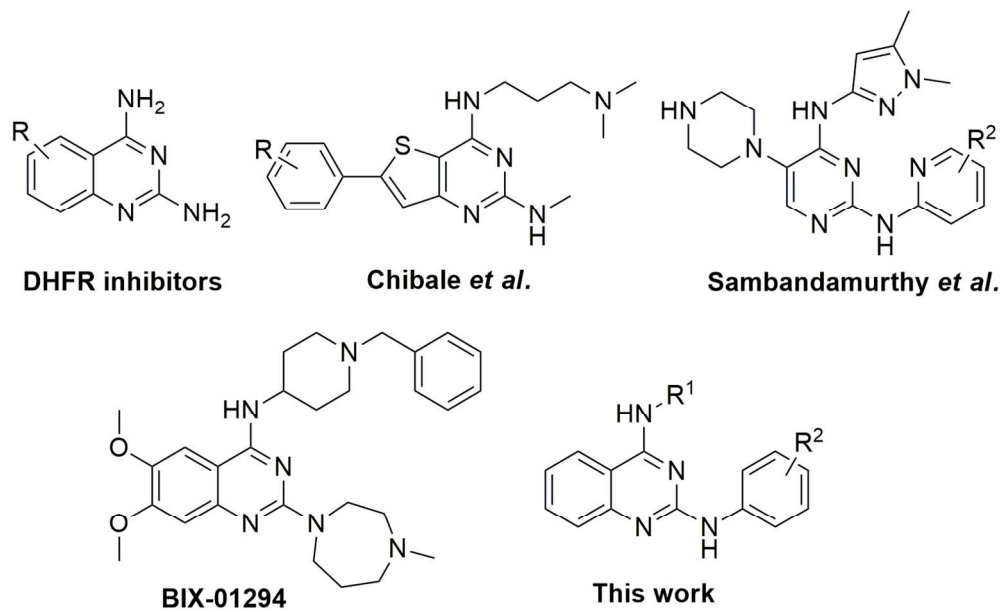


Figure 1.

133x81mm (300 x 300 DPI)

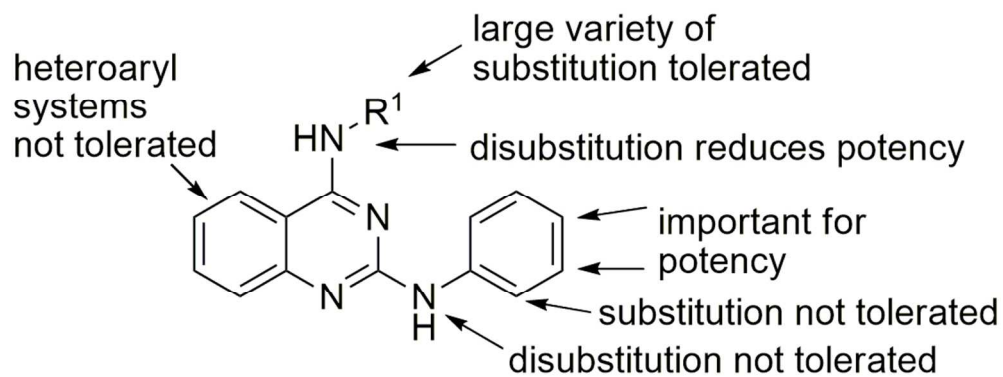


Figure 2.

95x36mm (300 x 300 DPI)

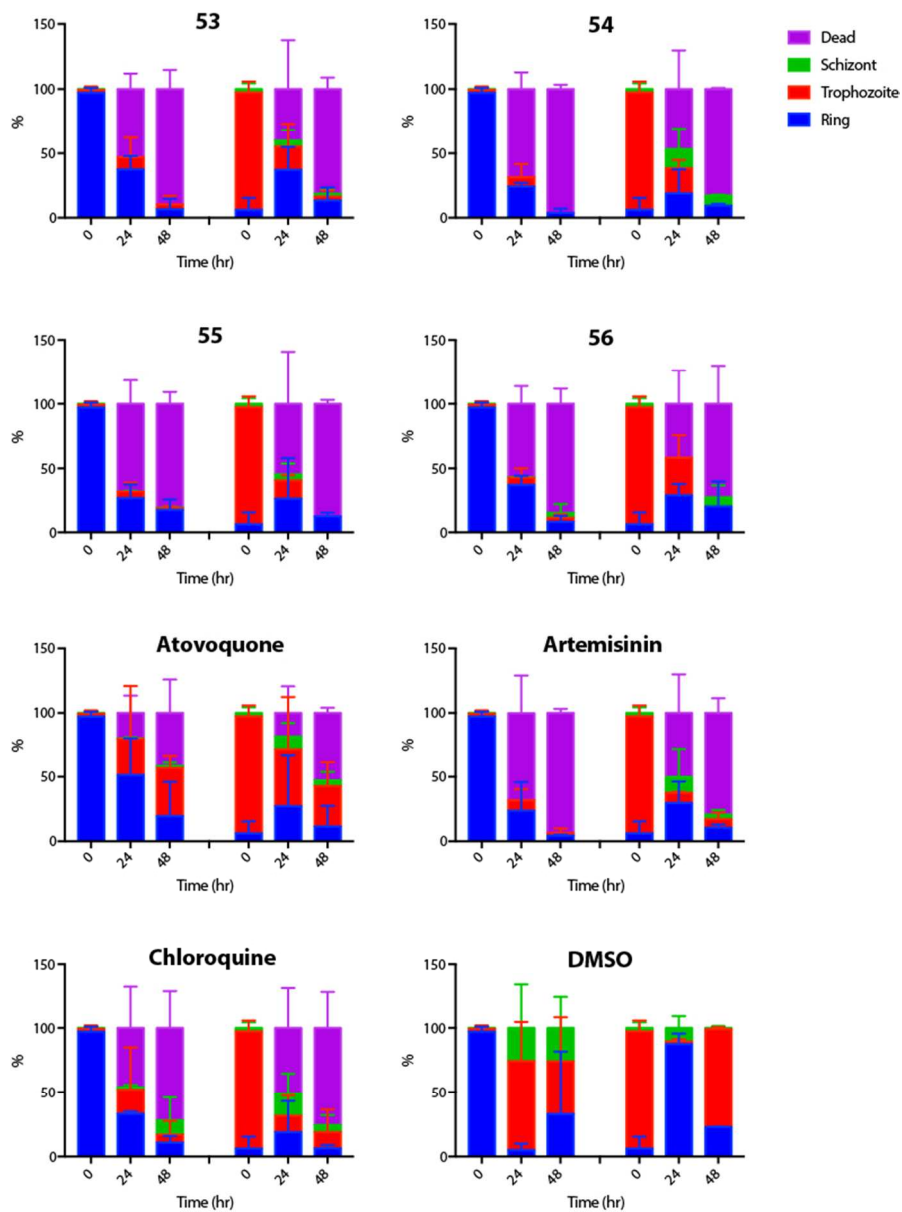


Figure 3.

133x180mm (150 x 150 DPI)

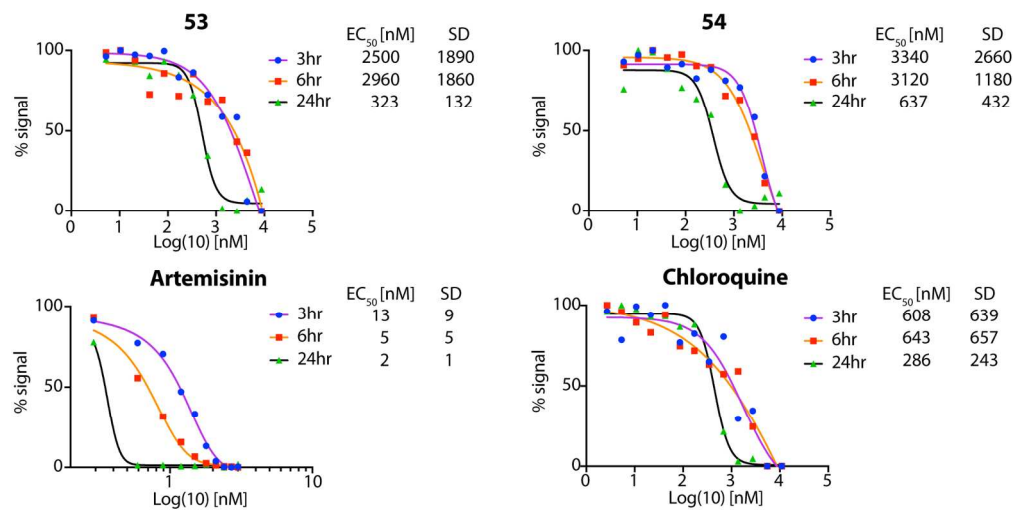


Figure 4.

152x78mm (300 x 300 DPI)

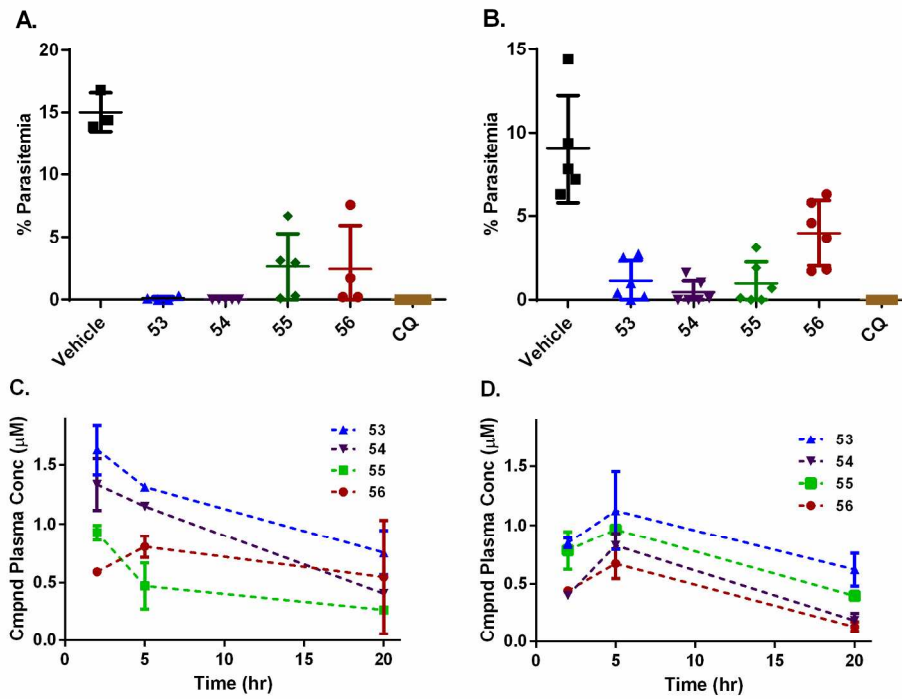


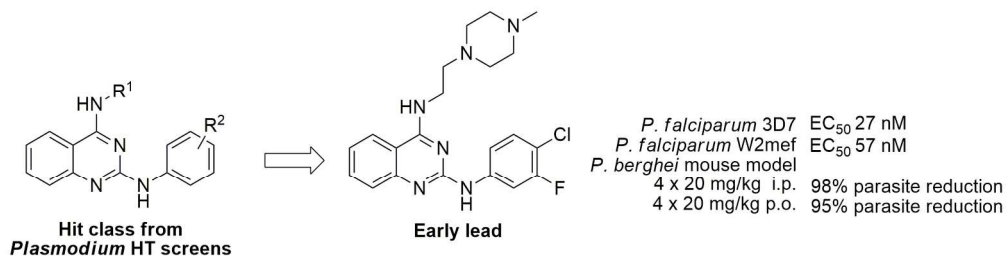
Figure 5.

199x155mm (300 x 300 DPI)



Scheme 1.

122x26mm (300 x 300 DPI)



TOC Graphic

187x47mm (300 x 300 DPI)